Superconducting $\beta(\beta')$-vanadium bronzes under pressure

Touru Yamauchi* and Yutaka Ueda
Material Design and Characterization Laboratory, Institute for Solid State Physics, University of Tokyo, 5-1-5 Kashiwanoha, Kashiwa, Chiba 277-8581, Japan

(Received 11 August 2007; revised manuscript received 7 November 2007; published 27 March 2008)

Since the first superconductivity in vanadium oxides was discovered in β-$Na_{0.33}V_2O_5$ under high pressure, β-vanadium bronzes have drawn much interest. In this paper, we report our current high-pressure studies on monovalent β-vanadium bronzes, β-$A_{0.33}V_2O_5$ (A=Li, Na, and Ag). The superconducting states are realized by suppressing the charge ordering states under high pressure in all monovalent β-vanadium bronzes, in contrast to divalent β-$A_{0.33}V_2O_5$ (A=Ca, Sr, and Pb). The superconducting phases adjacent to the charge ordering phases imply an important role of charge fluctuation for the superconductivity. The obtained pressure-temperature phase diagrams tell us that the superconducting states compete with not only charge ordering states but also new nonsuperconducting metallic states under high pressure. The superconducting states are very sensitive to A-cation nonstoichiometry, suggesting a close relation to the commensurability of carriers and a possibility of non s-wave superconductivity.

DOI: 10.1103/PhysRevB.77.104529 PACS number(s): 74.10.+v, 74.25.Dw, 74.62.Fj

I. INTRODUCTION

Discovery of new pressure-induced superconductivity has opened the gates to frontiers of condensed matter physics. The fascinating superconductivity in heavy fermion systems and in organic conductors was found under high pressure.[1,2] Pressure has a crucial advantage because it can change electronic properties without randomness effects.

Transition metal oxides, one major class of materials in highly correlated electron systems, have drawn much attention after the discovery of high-T_c superconducting cuprates (HTSCs). In short, the key to the high-T_c superconductivity (HTS) was hole doping to Mott insulators by chemical substitution.[3] This situation has caused fluorescence of doping study on transition metal oxides. Actually, chemical doping is a powerful method to control electronic states of the transition metal oxides and/or other compounds; however, it has another kind of influence; doped atoms inevitably induce random potential to the electron system, which makes the system complicated. On the other hand, pressure is free from such difficulties.

Although transition metal oxides frequently need relatively higher pressure to observe some pressure-induced phase switching rather than organic and/or heavy fermion systems do, recent improvements of high-pressure technique pave the way to capture drastic phase transitions of many kinds of transition metal oxides.

One of the typical examples is a series of vanadium oxides represented as a chemical formula β-$A_{0.33}V_2O_5$ (A=Li, Na, Ag, Sr, Ca, and Pb). These compounds which are called β-vanadium bronzes are quasi-one-dimensional (q1D) conductors. All of them except for β-$Pb_{0.33}V_2O_5$ show charge order type metal-insulator transition (MIT) as frequently observed in mixed valent binary vanadium oxides.[4–10] Among them, β-$Na_{0.33}V_2O_5$ was an epoch-making compound because it was found that it shows a peculiar pressure-temperature (P-T) electronic phase diagram where a superconducting (SC) phase competes with a charge ordering (CO) phase at around 7 GPa.[11]

Since this discovery of superconductivity in vanadium oxide, we have carried out high-pressure studies on all members of β-vanadium bronzes using highly hydrostatic pressure technique up to about 10 GPa as described below. As the results of these studies, we have observed pressure-induced superconductivity adjacent to the charge order in all monovalent A^{1+} (A=Li, Na, and Ag) compounds. On the other hand, it has been elucidated that all divalent A^{2+} (A=Ca, Sr, and Pb) compounds do not show any sign of superconductivity within the observed pressure-temperature region, although all of them show metallic conduction as well as the monovalent compounds.

The monoclinic crystal structure of β-$A_{0.33}V_2O_5$ consists of a characteristic V_2O_5 framework and A cations as illustrated in Fig. 1. The V_2O_5 framework is formed by $(V1)O_6$, $(V2)O_6$ octahedra, and $(V3)O_5$ pyramids, where V1, V2, and V3 are three distinct V sites. Each polyhedra forms infinite chains along the b axis (the q1D conduction axis). The A cations are located in the straight tunnels along the b axis and occupy only one of the two nearest-neighboring A sites in the same ac plane. Therefore, the stoichiometric composition of A cation is strictly 1/3, namely, 0.33. Incidentally, β' structure has a similar V_2O_5 framework to that of β structure, but A cations (A=Li and Cu) can occupy both sites of nearest-

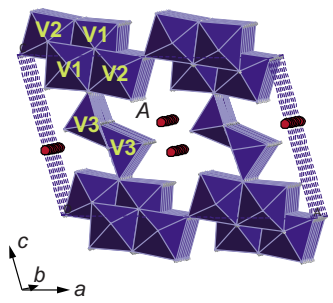

FIG. 1. (Color online) Crystal structure of β-vanadium bronzes. This view is a projection along the monoclinic b axis which is a direction of quasi-one-dimensional conduction.

neighboring A' sites (A' sites differ from A sites of β structure), giving the stoichiometric composition of 2/3; $\sim$0.66.[12,13]

As characteristics of β and β' structures, A-cation nonstoichiometry is well known and it crucially affects the electromagnetic properties of these compounds. For instance, even the MIT steeply disappears when the A-cation content becomes slightly off stoichiometric, $x \sim 0.30$ in β-$Na_xV_2O_5$.[4,5] We have also performed high-pressure study on slightly off-stoichiometric β-$Na_{0.32}V_2O_5$ and β-$Li_{0.38}V_2O_5$ crystals. The results will be presented and discussed later.

The major aim of this paper is to report the detailed results of Li compound and review the results of our current high-pressure studies on all monovalent β-vanadium bronzes, β-$A_{0.33}V_2O_5$ (A=Li, Na, and Ag). The detailed results of resistivity measurements under high pressure are reported and the electronic P-T phase diagrams are constructed from the results. We will report that all these compounds have pressure-induced SC phases adjacent to CO phases and show very similar P-T phase diagrams. The common characteristics in these P-T phase diagrams will be discussed in terms of the ground state competition and dimensionality, comparing with those of divalent (A=Ca, Sr) compounds and other typical compounds which show MIT. We will also discuss what is responsible for the superconductivity, taking the results of nonstoichiometric compounds and β'-$Cu_{0.65}V_2O_5$ into the consideration.

II. EXPERIMENT

To obtain hydrostatic pressure above 10 GPa, a cubic-anvil-type high-pressure apparatus was equipped with precisely scoured sintered diamond anvils. A technique using a droplike pressure medium surrounding a sample crystal was also applied in this study to ensure better hydrostatic pressure and to avoid damage of sample crystal. A drop of methanol-ethanol-water (16: 3: 1 in volume) mixture, as shown in Fig. 2, was used as a pressure medium. The out of droplike pressure medium was filled with the second pressure medium, Fluorinert, to prevent the evaporation of methanol-ethanol-water drop during long time experiments about several weeks.

The resistance under high pressure was measured along the b axis by ordinal four-probe method under several excitation currents to check its Ohmic behavior. To ensure the reliability of the electrical and mechanical contacts to sample crystal under pressure, four gold thin wires (15 μm diameter) were knotted to sample crystal (typically 0.4 mm long) and were fixed by gold paste (Tokuriki, Chem. No. 8560). These wired crystals were calcined at 500 °C in evacuated silica tube with large amounts of stoichiometric powder sample. Furthermore, the contacts were reinforced mechanically by epoxy silver paste (Epoxy Technology, H20S). To keep good electric contacts to sample crystal during long time experiments, the maximum applied voltage to sample crystal must be less than 0.5 V, especially in β-$Li_{0.33}V_2O_5$, because electrochemical reaction occurs at higher voltage and the electric contacts are damaged presumably due to Li-ion transfer to the electrodes.

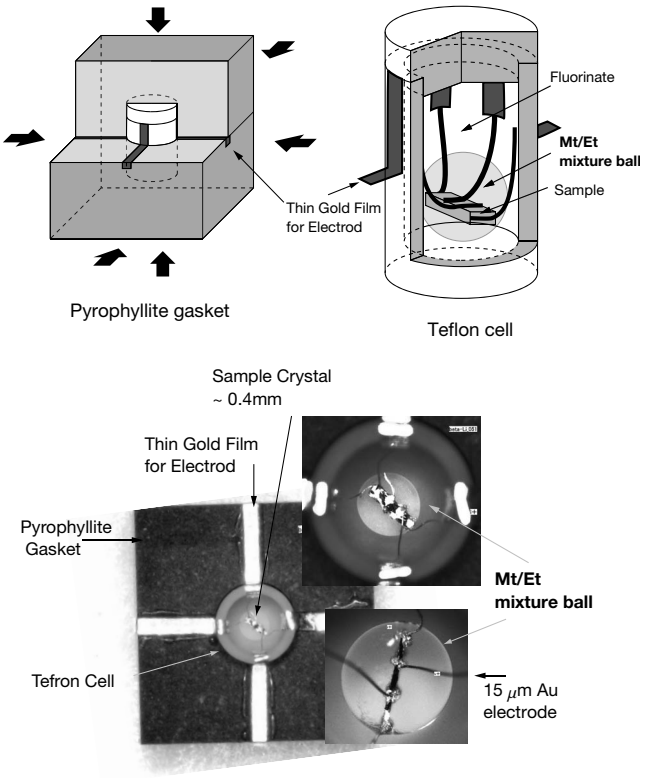

FIG. 2. Resistivity measurement setting for high pressure up to 12 GPa. To obtain better hydrostatic pressure, a sample crystal is surrounded by the pressure medium of methanol-ethanol-water mixture. This mixture is further covered with Fluorinert as the second liquid pressure medium. The diameter of Teflon cell is 1.5 mm.

The magnetic susceptibility measurement is one of the most powerful methods to observe the electromagnetic states of materials, nevertheless susceptibility measurements under pressure are quite restricted because the pressure cell has merely a quite small sample space. For instance, the sample space of a cubic-anvil-type pressure cell (effectively 0.8 mm ϕ and 0.8 mm length) has a capacity of primary-40 and/or secondary-40 turn pickup coils (0.5 mm ϕ, inner diameter), as shown in Fig. 3. Actually, superconductivity in β- and β'-vanadium bronzes was confirmed by measuring the ac susceptibility using the inductively coupled coils in cubic-anvil-type pressure cell. The coupled pickup coils are handmade with the thinnest Cu wire (35 μm ϕ) which is commercially supplied. In the measurement, ac susceptibility of the samples was detected as mutual inductance between the coupled coils by lock-in amplifier 5610B (NF Co. Ltd). The schematic electronic configuration for this measurement is also illustrated in this figure. This quite simple experimental system composed of pickup coils and a lock-in amplifier has enough sensitivity to detect superconducting and ferromagnetic transitions which show enormously large magnetic signals. In general, however, almost magnetic signals are too small to detect the transitions such as antiferromagnetic ordering by this method.

Here, we touch about sample crystal preparation, because A-cation stoichiometry of β-$A_xV_2O_5$ is very sensitive to sample preparation method. Sample crystals are grown in N_2

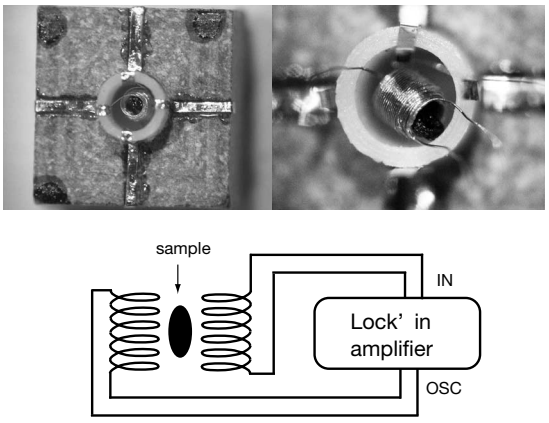

FIG. 3. ac-susceptibility measurement setup in a pyrophyllite gasket. The susceptibility is detected by mutual inductance of inductively coupled coils. The inner space of the coils is filled with a sample crystal and methanol-ethanol pressure medium. Out of the coils, Fluorinert is charged.

atmosphere by rf-heating Czochralski method using self-flux in a Pt crucible. As fluxes for A=Li, Na, and Ag compounds, $LiVO_3$, $NaVO_3$, and $AgVO_3$ were used, respectively, to prevent VO_2 from growing. By changing chemical composition (the ratio between an objective compound and a flux) in crucible, optimum growing conditions were investigated. In β-$Na_xV_2O_5$ and β-$Ag_xV_2O_5$, as-grown crystals were almost stoichiometric ($x\sim0.33$). On the other hand, as-grown β-$Li_xV_2O_5$ crystals were off stoichiometric ($x\sim0.38$). These compositions were determined by an inductively coupled plasma atomic emission spectrometer (ICP-AES). The Li concentration in the crystals can be tuned through the following preparation steps: (i) washing as-grown crystals in hot hydrochloric acid, and (ii) calcination of as-grown crystals with a large amount of powder sample of x=0.33 in evacuated quartz tubes at 600 °C for about 20 h. β-$Na_{0.32}V_2O_5$ crystals were also prepared by the calcination of crystals embedded in large amounts of x=0.32 powder sample in an evacuated quartz tube. Since the resolution of the chemical analysis is about 2%, such small difference of A-cation content between x=0.33 and x=0.32 is difficult to detect. Hence, we have characterized A-cation content of the sample crystals as nominal concentration of powder samples. We also characterized Na content of the crystals by checking the difference of the charge ordering temperature from the optimum temperature, 135 K in the stoichiometric crystal.[4,5]

III. RESULTS

A. Stoichoimetric compounds

In this section, the results of the stoichiometric monovalent β-vanadium bronzes β-$A_{0.33}V_2O_5$ (A=Li, Na, and Ag) are represented. Especially, the temperature dependences of resistivity (ρ-T curves) are checked, its reproducibility and consistency among these three compounds. Here represented ρ-T curves shows relevant behaviors which were not observed in previous works[11,14] probably due to an unsophistication of the experiments. These observations will be discussed in the later parts of this paper and lead us to insights of these compounds.

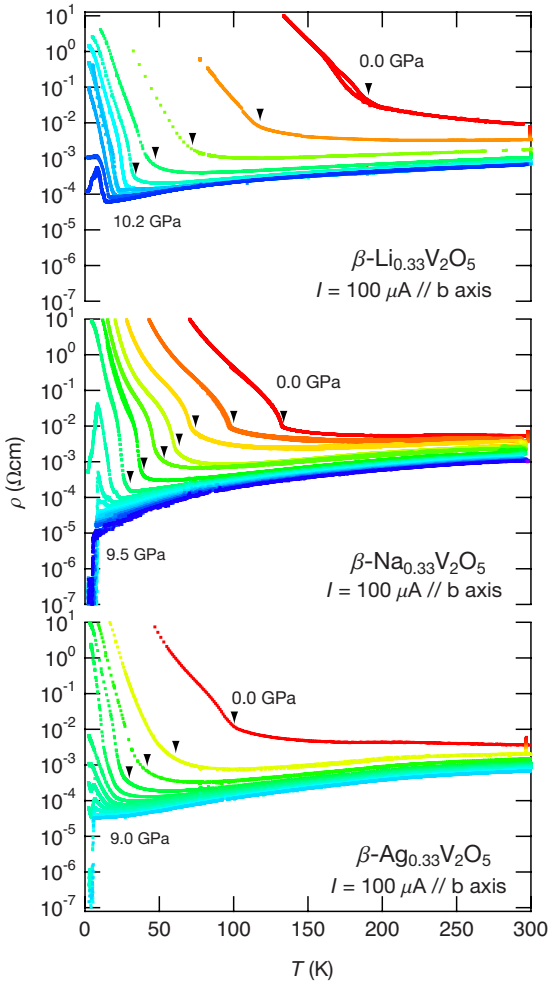

FIG. 4. (Color online) Temperature dependences of resistivity (ρ-T curves) for stoichiometric β-$A_{0.33}V_2O_5$ (A=Li, Na, and Ag) up to about 10 GPa. The charge order transitions are suppressed under pressure, as marked by an inverted triangle symbol and finally the superconducting behaviors (the drops in ρ-T curves) are observed in all compounds.

1. ρ-T curves under pressure in β-$A_{0.33}V_2O_5$, A=Li, Na, and Ag

The ρ-T curves under several pressures are exhibited for three stoichiometric monovalent compounds, β-$A_{0.33}V_2O_5$ (A=Li, Na, and Ag) in Fig. 4. Here, note that the resistivity (ρ) was measured along the b axis, q1D direction, in all compounds.

As shown in this figure, the charge ordering temperature T_{CO} marked by an inverted triangle symbol, where the ρ-T curve bends, decreases as increasing pressure in all compounds. Near the critical pressures (P_c=9.9, 7.0, 6.8 GPa for A=Li, Na, and Ag compounds, respectively) where the minimum absolute ρ value in the ρ-T curves (at just above the T_{CO}'s) reaches 100 $\mu\Omega$ cm, both sudden upturn by charge order and successive drop by superconductivity are observed

in the same ρ-T curve for all compounds. These critical behaviors will be discussed later. Here, P_c is defined as the pressure where the drop of ρ is observed, namely, the SC phase appears. With slightly increasing pressure above the P_c, the ρ-T curves show zero resistivity within experimental resolution except for Li compound. This experimental resolution is dominated by excitation current and noise level of the experimental setup ($\sim 10^{-8}$ V). The resistivity measurements suggest the SC phase is neighboring to the CO phase in all compounds.

In moderate-temperature range, 100–300 K, ρ-T curves of all these compounds in some pressure range show clear metallic behaviors ($d\rho/dT>0$), as shown in Fig. 4, where the ρ becomes smaller than the Mott-Ioffe-Regel limit.[15,16] On the other hand, in the case of larger ρ than Mott limit, some ρ-T curves naturally show temperature independent and/or weakly insulating behaviors ($d\rho/dT<0$) even at higher temperature than the T_{CO}. Here, the Mott limit, critical resistivity is estimated at about 2.6–1.9 mΩ cm by considering a free electron model for a layered two-dimensional (2D) system and it is given by the equation $\rho_c = hc_0/e^2 \cdot 1/k_F l$ ($k_F l = 1$),[17] where c_0 shows the distance between layers. Note that the absolute values of the observed resistivity have some errors within factors 2 or 3 mainly due to the difficulty to estimate the quite small sample dimensions precisely.

At present, there is no definite evidence for 2D conduction of β-vanadium bronzes at high pressure ($\sim$7 GPa); however, some observations imply an occurrence of dimensional crossover from q1D to quasi-two-dimensional (q2D) systems with increasing pressure as discussed in the later parts of this paper. It is naturally supposed that these conduction layers are the *ab* and/or *bc* planes, thus the c_0 can be estimated at 9.9 Å (*ab* plane) and/or 7.3 Å (*bc*) by crystallographic considerations.

It should be noted that the SC phase appears when the conductance becomes about $k_F l \sim 20$ (corresponding to 100 $\mu\Omega$ cm). This value is relatively lager than that ($k_F l \sim 4$) observed in $La_{2-x}Sr_xCuO4$ system.[18] This probably implies larger coherent length ξ of Cooper pair in β-vanadium bronzes than that in HTSC, which is consistent with the relatively low SC transition temperatures, $T_{SC} \sim 8.5$, 8.0, and 6.5 for Li, Na, and Ag compounds, respectively.

2. Superconductivity beyond charge ordering

To certify the appearance of superconductivity, ac-susceptibility measurements were carried out using coupled coils via a sample crystal and a lock-in amplifier as explained in the previous section (see Fig. 3).[11] In the experiments, the mutual inductance between primary and secondary coils was observed, expecting that floating capacitance should not change with temperature sweeping. This means the observed change of the mutual inductance should be attributed to the change of ac susceptibility of the sample crystal. The ac susceptibility around the superconducting transition of Pb metal was also observed as a reference, using geometrically same coupled coils.

The results of ac-susceptibility, $\chi(\omega)$ measurements ($\omega \sim 534$ Hz) in β-$Na_{0.33}V_2O_5$ under several pressures (5.0–9.5 GPa) are shown in Fig. 5(a). These $\chi(\omega)$-T curves have already appeared in Ref. 11. The ρ-T curves (linear plots) of similar P-T region are also exhibited in panel (b). The sample crystal was inserted in the pickup coils along the *b* axis, thus the observed $\chi(\omega)$ should be the component along the *b* axis. Furthermore, it should be noted that $\chi(\omega)$ was measured at almost zero external magnetic field. Panel (a) shows the temperature dependences of the inductance (lock-in output) between field and pickup coils, which should correspond to the temperature dependences of the real part of ac susceptibility [$\chi(\omega)$-T curves].

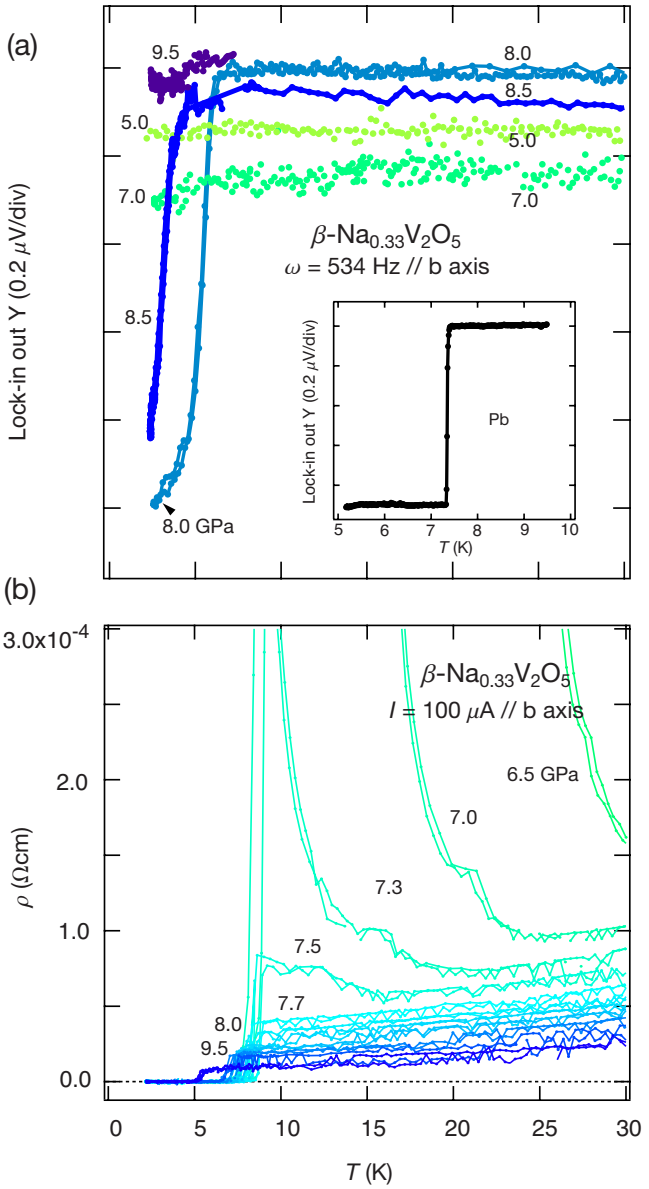

FIG. 5. (Color online) (a) Temperature dependences of ac susceptibility [$\chi(\omega \sim 534$ Hz)-T curves] under several pressures (5.0–9.5 GPa) for β-$Na_{0.33}V_2O_5$. These data already appeared in Ref. 11. The inset shows ac susceptibility around the superconducting transition of Pb metal measured by the same method as a reference. (b) The ρ-T curves around the superconducting transition for β-$Na_{0.33}V_2O_5$.

A substantial sharp drop in $\chi(\omega)$-T curve was observed at 8.0 GPa and at 6.5 K. This observation clearly certifies the SC shielding effect, namely, the appearance of SC phase at 8.0 GPa. Using a simple proportional calculation, assuming that Pb metal has 100% SC volume fraction, the SC signal in $\chi(\omega)$ corresponds to about 70% SC volume fraction. However, it should be noted that such a large signal can be obtained in the case of geometrically favorable distribution of few percent of superconducting phase for this ac susceptibility measurement. As well known, the real SC volume fraction can be revealed by dc magnetization and/or specific heat measurements, which needs intensive improvements of high-pressure experimental technique. Despite this situation, the two facts: an absence of SC signal in $\chi(\omega)$ at 7 GPa where the ρ-T curve reaches to zero resistivity and an appearance of intensive SC signal in $\chi(\omega)$ at 8 GPa, demonstrate rapid growing of SC phase with slight increasing pressure. Thus we can expect a massive SC ground state beyond the CO phase. The features near P_c will be discussed in the later sections.

On the other hand, the $\chi(\omega)$-T curves do not show any anomaly at the CO transition; nevertheless, MIT is clearly observed in ρ-T curves as shown in panel (b). This probably means that the susceptibility anomaly at T_{CO} is considerably smaller than that at T_{SC}. Actually, the anomaly on $\chi(0)$-T curve at T_{CO} is slightly observed at ambient pressure even by a very sensitive magnetometer, superconducting quantum interference device.

Here it should be emphasized again that both ac-susceptibility and resistivity measurements in Figs. 5(a) and 5(b) proved the pressure-induced superconductivity in β-$Na_{0.33}V_2O_5$. A disagreement between the onset temperatures of SC transition observed in resistivity (8.0 K) and in ac-susceptibility (6.5 K) measurements at 8 GPa is frequently observed in oxide superconductors as reported in the literatures.[19] On the other hand, the observed onset temperature in susceptibility coincides with the offset temperature in resistivity for β-$Na_{0.33}V_2O_5$.

In contrast to Na and Ag compounds, the ρ-T curve of Li compound clearly shows a drop but ρ does not become zero resistivity near the P_c, as shown in Fig. 4. To certify the appearance of superconductivity in Li compound, magnetic field dependence of ρ-T curve at 10.1 GPa was examined. As shown in Fig. 6, the observed ρ-T curves up to 3.0 T clearly show significant magnetic field dependence; only the temperatures where ρ-T curves drop shift lower with increasing magnetic field and the parts of ρ-T above the drop do not show field dependence. This feature strongly suggests the appearance of SC phase at this pressure. From the results, the magnetic field dependence of SC transition temperature dT_{SC}/dH was estimated at about −0.74 K/T.

At present, it is impossible to control the direction of the sample crystal to the applied magnetic field because of the experimental configuration. In compressing process, a sample crystal surrounded by liquid pressure medium frequently changes its direction in the pressure cell. Thus, it is too simple to compare this field dependence of T_{SC} with that of other pressure-induced superconducting oxide, $Sr_2Ca_{12}Cu_{24}O_{41}$,[20,21] and organic one, $(TMTSF)_2PF_6$.[22] However, we dared to compare each field dependence dT_{SC}/dH and found an intermediate value between the strongest and weakest one in both oxide (−0.2 to −1.0 K/T) and organic (−0.3 to −3.6 K/T) systems.

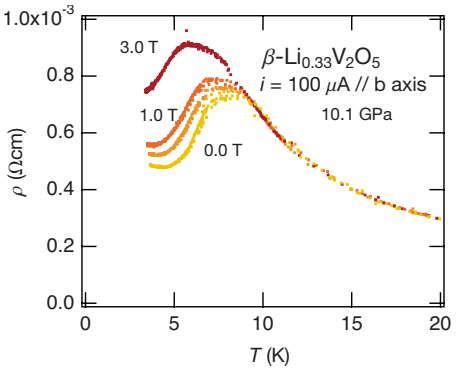

FIG. 6. (Color online) Magnetic field dependence of ρ-T curves at 10.1 GPa, near P_c in β-$Li_{0.33}V_2O_5$. The observed ρ-T curves up to 3.0 T clearly show strong magnetic field dependence, which is an evidence for the appearance of superconducting phase at this pressure.

The observation of magnetic field dependence is a good evidence for existence of the superconductivity at P_c where the charge order is about to collapse; however, Li compound does not show simple behaviors observed in Na and Ag compounds. This is presumably due to the appearance of other phase which breaks the superconductivity around P_c. The existence of a nonsuperconducting new higher-pressure phase (NP) will be discussed later on.

3. Phase coexistence around the critical pressure

To show critical behaviors at the phase switching from CO to SC phases, the detailed ρ-T curves of Na and Ag compounds near the P_c are exhibited in Fig. 7. These two graphs are simply macrographs of the low-temperature part of Fig. 4. The sudden drops of ρ which are marked by small black inverted triangles in this figure are observed at 7.0 GPa (Na) and 6.8 GPa (Ag), and the zero resistivity (within the experimental resolution) is observed at 7.3 GPa (Na) and 7.5 GPa (Ag), respectively. Differing from the Li compound, both Na and Ag compounds show typical SC metallic behaviors.

However, the details of ρ-T curves around the P_c are different between Na and Ag compounds. In Na compound, only one ρ-T curve at 7.0 GPa shows moderate drop to nonzero resistivity as observed in Li compound. With further increasing pressure only up to 7.3 GPa, the ρ-T curve shows a sharp drop to zero resistivity with a typical transition width ~1.5 K. On the other hand, an anomalous behavior as "cranked ρ-T curves" is observed at the superconducting transition in Ag compound (see the ρ-T curves at 6.8–7.3 GPa, typically at 7.0 GPa). Such cranked ρ-T curves near the P_c were always observed in three different experimental runs on Ag compounds, while such a peculiar ρ-T curve was never observed on Na compound even in the three runs.

This difference and peculiar behaviors in the two compounds are probably explained by an inhomogeneity which

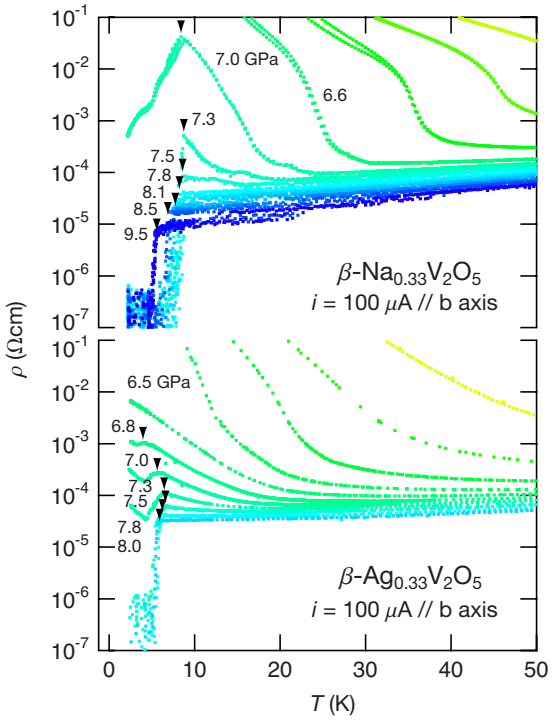

FIG. 7. (Color online) Pressure dependence of ρ-T curves in β-$Na_{0.33}V_2O_5$ and β-$Ag_{0.33}V_2O_5$ below 50 K. The behaviors of ρ-T curves clearly show that the superconducting transition is different between β-$Na_{0.33}V_2O_5$ and β-$Ag_{0.33}V_2O_5$. The relatively sharp drop in ρ-T curve shows homogenous hydrostatic pressure generated in the experiments.

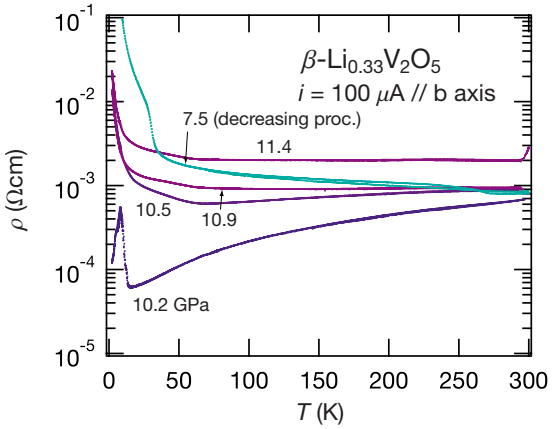

FIG. 8. (Color online) ρ-T curves of β-$Li_{0.33}V_2O_5$ measured above the critical pressure, 10.2 GPa and at 7.5 GPa in a pressure decreasing process. With slightly increasing pressure from 10.2 to 10.5 GPa, the whole aspects on the ρ-T curve, charge ordering, superconducting transitions, and further metallic behavior, suddenly disappear. This implies the existence of a new phase above 10.5 GPa which breaks superconductivity.

arises from a coexistence of CO and SC phases (probably macroscopic) near the phase boundary. Such a coexistence is generally an evidence for first-order transition between CO and SC phases. Assuming the phase coexistence occurs in a striped manner perpendicular to the b axis (current direction of the measurements), the cranked behavior in Ag compound can be explained by electrical serial connection of SC and CO parts in the crystal. Different behaviors between Na and Ag compounds near the P_c might be attributed to different manner of the phase coexistence. On the other hand, there is another possible explanation for the inhomogeneity, that is, very slight fluctuation of A-cation content in the sample crystal. As mentioned later, the superconductivity disappears in slightly off-stoichiometric β-$Na_{0.32}V_2O_5$ crystal. This means very tiny uncontrollable fluctuation of chemical composition results in a phase coexistence of CO and SC phases, if P_c is crucially affected by the chemical compositions. In this case, it is difficult to say something about the order of the transition between CO and SC phases.

In this paper, a term "coexistence" will express macroscopic coexistence hereafter. This means that both SC and CO phases appear simultaneously and inhomogeneously on a macroscopic scale. Besides, it still be unknown at present whether microscopic phase coexistence intensively studied in heavy fermion and/or organic systems[23,24] is likely in β-vanadium bronzes or not.

The coexistence of SC and CO phases cannot be attributed to the inhomogeneity of pressure. In Ag compound, the transition width of superconducting transition is about 1.0 K at 6.8 GPa. At this pressure, the pressure dependence of T_{SC} is relatively large ($\sim +9.2$ K/GPa; the onset temperature where the ρ-T curve shows drop is 4.01 K at 6.8 GPa and 5.95 K at 7.0 GPa). This means that the transition width would be about 9 K, if the pressure inhomogeneity were 1 GPa. From simple calculation taking the observed transition width and the pressure dependence of the T_{SC} into account, the pressure inhomogeneity is estimated at about 0.12 GPa. This is quite smaller than the width of the coexistence pressure region, 6.8–7.5 GPa.

4. New nonsuperconducting higher-pressure phases

The highest pressure in our pressure apparatus is about 13 GPa at present. For generating such high pressure, we have employed sintered diamond anvils equipped with the cubic-anvil-type pressure apparatus. Figure 8 represents the ρ-T curves of β-$Li_{0.33}V_2O_5$ observed in the highest-pressure region: four ρ-T curves measured in a sequence, 10.2 $\rightarrow$ 10.5 $\rightarrow$ 10.9 $\rightarrow$ 11.4 GPa and one ρ-T curve at 7.5 GPa in a pressure decreasing process. The ρ-T curves are different between 10.2 GPa and above that. The ρ-T curve at 10.2 GPa clearly shows both a sharp CO upturn at 15.5 K and a sharp SC drop at 8.5 K. This SC nature steeply disappears with slightly increasing pressure only up to 10.5 GPa. Furthermore, the tendency of pressure dependence of overall ρ-T curve drastically changes at around the critical pressure. Below 10 GPa, ρ-T curves shift downward (low ρ) as increasing pressure, as shown in Fig. 4. On the other hand, the curves above 10 GPa shift upward (high ρ) with increasing pressure, as exhibited in Fig. 8. The ρ-T curves at 10.5, 10.9, and 11.4 GPa are qualitatively the same; very narrow gap semiconductinglike behavior without SC nature.

These drastic changes with slightly increasing pressure just above P_c imply sudden appearance of a new phase (NP phase) with a non-SC ground state around 10 GPa in

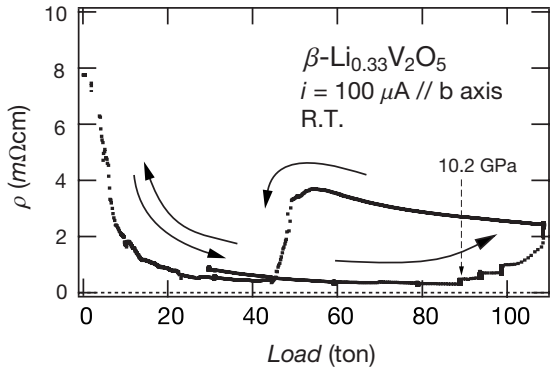

FIG. 9. A compressing curve of resistivity (ρ-load curve) in β-$Li_{0.33}V_2O_5$ at room temperature. As increasing pressure, resistivity monotonically decreases up to about 10 GPa and then increases, showing minimum at this pressure. Observed large hysteresis implies any crystallographical phase transition around 10 GPa. The estimated width of the hysteresis loop is about 3.0 GPa.

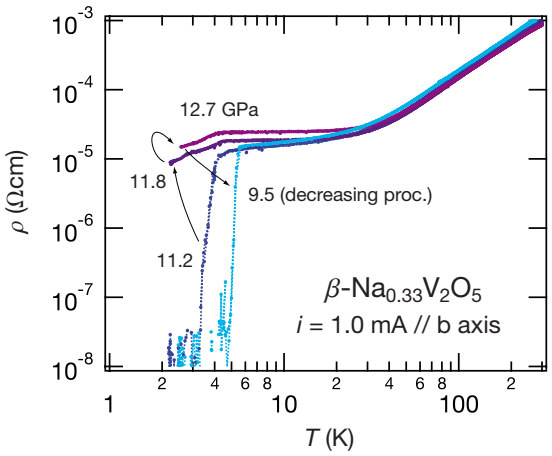

FIG. 10. (Color online) ρ-T curves of β-$Na_{0.33}V_2O_5$ measured above 11 GPa and at 9.5 GPa in a pressure decreasing process. The superconducting behavior drastically disappears between 11.2 and 11.8 GPa. The moderate drop in ρ-T curves above 11.8 GPa implies coexistence of superconducting and nonsuperconducting phases. A sharp drop of ρ-T curve at 9.5 GPa in a pressure decreasing process excludes an extrinsic origin of the moderate drop above 11.8 GPa such as crack of the sample crystal.

β-$Li_{0.33}V_2O_5$. The NP phase seems to appear above room temperature, because the two ρ-T curves of 10.2 and 10.5 GPa are crucially different in the whole temperature region below room temperature. This is also demonstrated by resistivity as a function of compressing (resistivity-load, ρ-L curve) at room temperature, as shown in Fig. 9. With increasing pressure, namely, as increasing applied load, the ρ decreases and shows broad minimum at around 10 GPa (95 tons) followed by a continuous increase up to 11.4 GPa (110 tons). The pressure about 10 GPa around the minimum is very close to the pressure where the NP phase appears. Then the measurements with decreasing pressure were carried out slowly, ~ -0.5 ton/h, to avoid a fracture of the sample crystal. With decreasing pressure from 11.4 GPa, the ρ slightly increases and then suddenly decreases to the value observed in a pressure increasing process around 50 tons; namely, the ρ-L curve shows a considerably large hysteresis loop. This hysteresis behavior excludes an extrinsic origin of the upturn of ρ above 10 GPa such as microcracks of the sample crystal. Such microcracks might be generated when the pressure medium freezes under high pressure (>10 GPa) at room temperature. However, if microcracks were in the sample crystal, the ρ would never recover, namely, ρ-L curve would never show such hysteresis loop. Therefore, this loop of ρ-L curve crucially demonstrates the appearance of NP phase above 10 GPa.

Here it should be noted that the calibration between pressure and compressing load does not work in a pressure decreasing process. However, the hysteresis width can be estimated by observing ρ-T curve at the load just below the hysteresis loop. The ρ-T curve observed at 48 tons in a pressure decreasing process is shown in Fig. 8 as ρ-T curve at 7.5 GPa. The ρ-T curve clearly shows CO transition at $T_{CO}=33$ K. From $T_{CO}=33$ K, the actual pressure can be estimated at 7.5 GPa. Thus, we found the hysteresis width about 3.0 GPa.

In β-$Na_{0.33}V_2O_5$, such a non-SC NP phase was also observed; however, the behaviors of ρ-T curve were considerably different from those in β-$Li_{0.33}V_2O_5$, as shown in Fig. 10. This figure exhibits four ρ-T curves in the following sequence: $11.2 \rightarrow 11.8 \rightarrow 12.7 \rightarrow 9.5$ GPa. The pressure of 9.5 GPa in a pressure decreasing process was determined from the pressure at which ρ-T curve in the pressure increasing process showed the same T_{SC}. The SC phase disappears with increasing pressure from 11.2 to 11.8 GPa. The ρ-T curves at 11.8 and 12.7 GPa show clear and moderate drops to nonzero resistivity as frequently observed in the critical pressure region between CO and SC phases. This implies coexistence of SC and non-SC metallic phases at the pressure region, 11.8–12.7 GPa. However, there is no crucial difference of overall behaviors of ρ-T curves in the normal metallic states in contrast to the case of β-$Li_{0.33}V_2O_5$. It should be noted that the optical study on β-$Na_{0.33}V_2O_5$ under high pressure also revealed the appearance of an unknown new phase above 12 GPa.[25]

From these results, we suppose that there exist non-SC high pressure phases as a common aspect of β-vanadium bronzes and these phases should be a key for the presence ans/or absence of superconductivity as discussed later.

5. P-T phase diagrams

The relationship among charge ordering (CO), normal metallic (NM), superconducting (SC), and nonsuperconducting higher pressure (NP) phases in β-$A_{0.33}V_2O_5$ (A=Li, Na, and Ag) is shown in Fig. 11 as the pressure-temperature (P-T) electronic phase diagrams of the three stoichiometric compounds. Note that these phase diagrams are represented with a linear scale of temperature and pressure, differing from those in the previous publications.[11,26] We have performed high-pressure experiments for each compound several times. As the results of sample dependence presumably due to very slight deviation of A-cation composition from the stoichiometry, the phase boundary was forced to scatter in these phase diagrams.

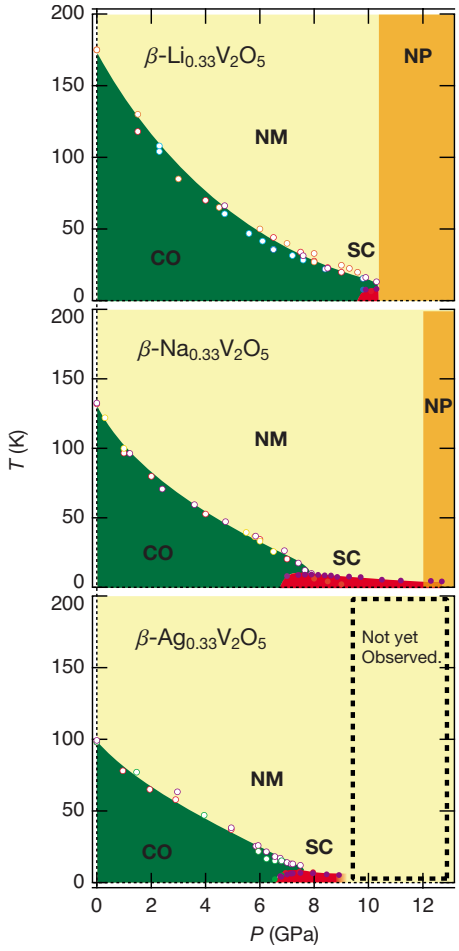

FIG. 11. (Color online) The pressure-temperature (P-T) electronic phase diagrams for β-$A_{0.33}V_2O_5$ (A=Li, Na, and Ag). Notations "CO," "SC," "NM," and "NP" represent charge ordering, superconducting, normal metallic, and newly observed higher pressure phases, respectively. These notations also appear in the main text. The different colors (online) of the symbols which represent T_{CO} and T_{SC} correspond to the different experimental runs, showing some discrepancy dependent on the samples.

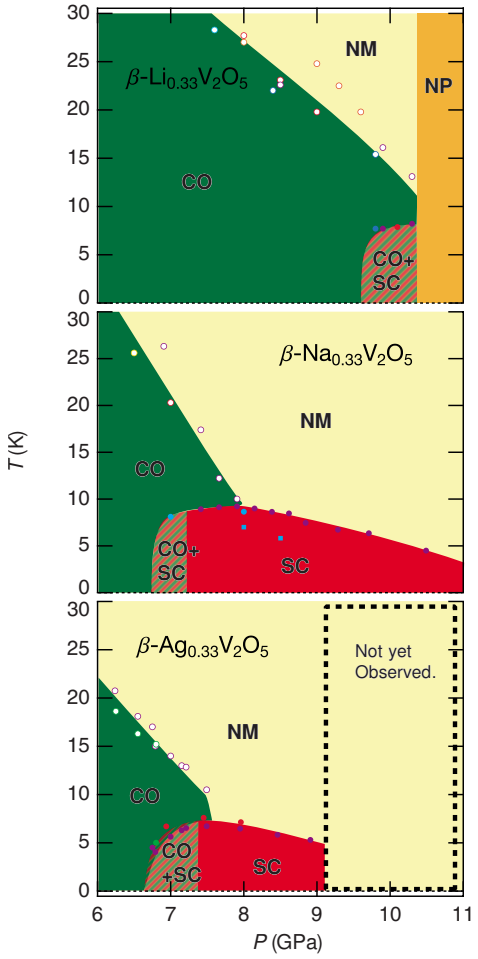

FIG. 12. (Color online) The macrographs of P-T phase diagrams in Fig. 11. Notations CO, SC, NM, and NP have the same meanings in Fig. 11. A hatched area with CO+SC means the region where ρ-T curves show moderate drops to nonzero resistivity. This behavior is probably due to the coexistence of SC and CO phases. The small square symbols (Na compound) represent T_{SC} determined from ac-susceptibility measurements.

The overview of these phase diagrams clarifies the following aspects: (i) CO phases are suppressed by pressure and SC phases appear adjoining CO phases; (ii) the phase boundary between NM and CO phases has a concave shape in all phase diagrams instead of an ordinary convex shape, which is discussed later; and (iii) the most noteworthy common aspect is that the phase boundary between NM and CO phases seems to terminate at the optimum point of SC phase. This implies an important role of charge fluctuation for the superconductivity.

Meanwhile, there is an important difference among these phases diagrams; substantially different pressure ranges for SC phases. It is wide in both Na and Ag compounds while narrow in Li compound. This is probably caused by the relationship between CO and NP phases, namely, it depends on how far NP phase exists from CO phase in P-T phase diagram. In Li compound, NP phase appears before CO phase vanishes completely and SC phase progresses fully.

As already mentioned, the phase boundary between NM and NP phases is considered to be parallel to the temperature axis in Li and Na compounds. To observe any crystallographic transitions between NM and NP phases, we are planning synchrotron radiation experiments using diamond anvil cell for both Li and Na compounds. At this stage, we suppose the NP phases in Li and Na compounds have different kinds of nature, and semiconductive (Li) and metallic (Na) conduction properties. It should be emphasized that the appearance of these NP phases is closely related to the presence and/or absence of SC phase in whole stoichiometric β-vanadium bronzes.

To make the phase relation around the P_c clear, the macrographs of the P-T phase diagrams near the P_c are shown in Fig. 12. Here the hatched area with a notation "CO+SC" shows a coexisting region of SC and CO phases where ρ-T curves show drops but do not reach to zero resistivity. If the fraction of SC phase is beyond a percolation limit, the SC paths are linked together and the sample crystal shows zero resistivity. Thus, the CO+SC region presented here should

be minimum in the coexisting region, in other words, the real coexisting region should be wider than the presented area. On the other hand, the bulk nature of the SC phase in Na compound was definitely expected by ac-susceptibility measurements[11] as discussed above. The T_{SC} observed by these susceptibility measurements are also plotted by small square symbols in the middle panel of Fig. 12. Relatively large discrepancy, ~2 K between T_{SC}'s derived from the onset of the ρ-T and $\chi(\omega)$-T curves, has been frequently observed in high-pressure studies. Incidentally, the T_{SC}'s from $\chi(\omega)$-T curves well coincide with the offset temperatures where the ρ-T curves reach zero resistivity. Moreover, a bulk SC phase is expected to appear at 8.0 GPa in Na compound where the upturn behavior in ρ-T curve completely disappears. This fact allows us to suppose the bulk superconductivity appears when the CO phase is completely suppressed by high pressure.

The pressure dependence of antiferromagnetic (AF) ordering transition temperature T_N and A-cation ordering temperature T^* were investigated in Na compound in the range up to 1.2 GPa using a piston cylinder-type pressure cell and up to 3 GPa using diamond anvil cell (DAC), respectively. Both T_N and T^* increase moderately, T_N: 24 K (0 GPa) to 31 K (1.2 GPa), T^*: 250 K (0 GPa) to 300 K (3 GPa). They, however, are not shown in the phase diagrams. A recent preliminary NMR study at 6 GPa revealed the absence of magnetic ordering down to 2 K in Na compound. The precise NMR study under high pressure beyond P_c is desired, because what ground state is adjacent to SC phase is crucial to discuss the superconducting mechanism.

B. Off-stoichiometric compounds

In this section, some results of high-pressure studies in off-stoichiometric compounds, *underdoped* β-$Na_{0.32}V_2O_5$ and β-$Li_{0.32}V_2O_5$ and *overdoped* β-$Li_{0.38}V_2O_5$, are represented, together with that in β'-$Cu_{0.65}V_2O_5$.

1. Underdoped compounds

We prepared slightly deficient samples of β-$Na_{0.32}V_2O_5$ and β-$Li_{0.32}V_2O_5$. The A-cation deficiency not only changes the valence state of V_2O_5 framework but also introduces randomness into the host electronic state. The ρ-T curves under high pressures are exhibited in Fig. 13 for Na poor (a) and for Li poor (b) samples, respectively. Note that the exhibited temperature range is 0–300 K for Na and 0–50 K for Li. In both samples the distinct CO transition was observed and it was suppressed by high pressure as in the stoichiometric samples. Similar to the case of the stoichiometric samples, the absolute value of the ρ became enough small ($k_F l \sim 20$) and the T_{CO} became enough low (<15 K). Nevertheless neither β-$Na_{0.32}V_2O_5$ nor β-$Li_{0.32}V_2O_5$ showed SC nature. These results show that the superconductivity is more sensitive to A-cation off stoichiometry and/or randomness than the charge order. The behaviors of ρ-T curves above critical

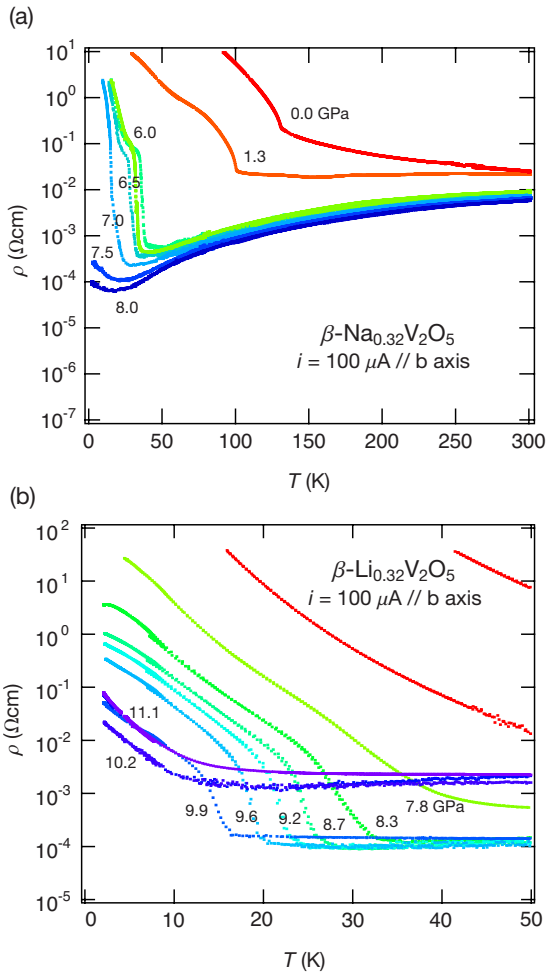

FIG. 13. (Color online) ρ-T curves under various pressures for nonstoichiometric (under doped) compounds: (a) β-$Na_{0.32}V_2O_5$ and (b) β-$Li_{0.32}V_2O_5$.

pressures are a little bit different between both samples, which is due to the different properties of NP phases, as described in the previous section.

As well known, in conventional superconductors, nonmagnetic impurities and randomness little affect the SC transition temperature T_{SC}. For example, noncrystalline lead has exactly the same T_{SC} as the crystalline one. On the other hand, in HTSC, slight amount of impurity such as Zn and Ni (both magnetic and nonmagnetic) in Cu site crucially decreases T_{SC}. Typically, only 3% impurity destroys the SC phase in $La_{2-y}Sr_yCu_{1-x}M_xO_4$ (M=Ni, Zn, $y \sim 0.15$, $x \sim 0.03$). Such sensitive nature of HTSC to impurity is regarded as a characteristic of d-wave superconductivity. Note that the superconductivity suffers significant damage only when on-site Cu ions in CuO_2 plane are substituted by the impurity ions. Moreover quite sensitive superconductivity to off-site[27] and on-site impurities[28,29] has been reported on the spin triplet oxide superconductor Sr_2RuO_4. In this system, both magnetic and nonmagnetic impurities of only 0.2% break the superconductivity. The observed off-stoichiometry effects on the superconductivity in β-vanadium bronzes remind us the case in $Sr_{2-y}La_yRuO_4$.

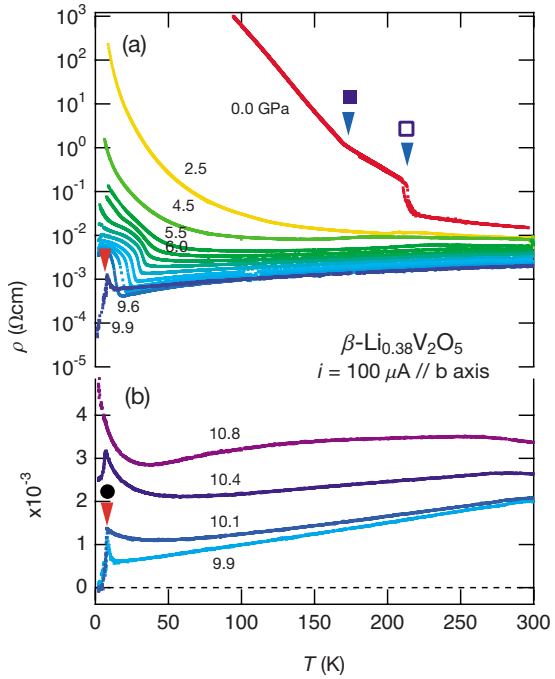

FIG. 14. (Color online) ρ-T curves of off-stoichiometric β-$Li_{0.38}V_2O_5$ up to 11 GPa. The ρ-T curves are divided into two groups: (a) the curves in 0.0–9.9 GPa with a semilog plot and (b) the curves in 9.9–10.8 GPa with a linear plot.

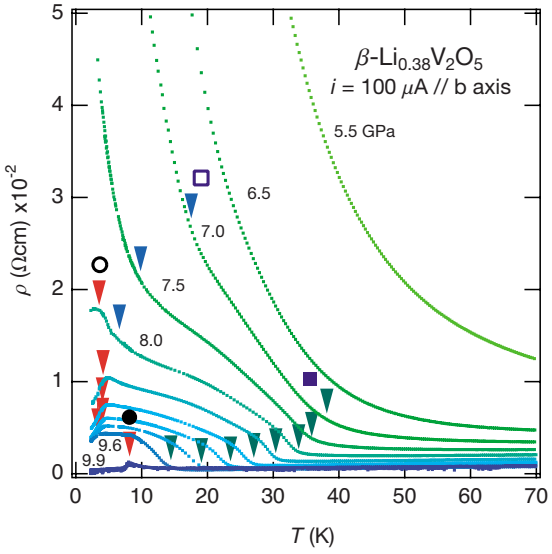

FIG. 15. (Color online) The macrograph of Fig. 14(a) with linear plot. The inverted triangles show anomalies in the ρ-T curves including SC transition. The complex behaviors are presumably attributed to the coexistence of β and β' phases, both which have similar V_2O_5 framework. The several kinds of symbols such as open and/or solid squares and circles also appear in the phase diagram exhibited later in Fig. 18.

2. Overdoped compound

One of the advantages of β-vanadium bronzes is chemical variety. In the case of β-Li system, it was accidentally discovered that Li ion can be tuned to relatively large excess content, namely, overdoped composition of $x=0.38$ (analyzed by ICP-AES). This was probably realized by long time contact between growing crystals and Li-rich molten substance in the crucible.

The ρ-T curves of the overdoped, β-$Li_{0.38}V_2O_5$ are shown in Figs. 14 and 15. Figure 14 exhibits (a) overall (0–300 K) curves with a semilog plot up to 9.9 GPa and (b) overall curves with a linear plot in 9.9–10.8 GPa. Figure 15 also shows ρ-T curves with a linear plot in 5.5–9.9 GPa below 70 K. The behaviors of overdoped, Li-rich nonstoichiometric compound are quite complex.

The significant results are summarized as follows.

(1) The ρ-T curve at ambient pressure shows a large jump at 220 K associated with a MIT and a small kink at 180 K [Fig. 14(a)].

(2) The ρ-T curves show clear drops at around 4.5 K but nonzero resistivity in 7.5–9.6 GPa (Fig. 15).

(3) The ρ-T curve shows a sharp drop at 8.5 K and zero resistivity by slightly increasing pressure from 9.6 to 10.1 GPa. However, the SC nature steeply disappears with slightly increasing pressure merely up to 10.4 GPa [Fig. 14(b)].

Although almost ρ-T curves do not show zero resistivity except the curve at 10.1 GPa, the origin of observed drops can probably be attributed to SC transition. Here it should be noted that the ρ-T curves of β-$Li_{0.38}V_2O_5$ have four characteristic temperatures of 220 and 180 K associated with CO transition and 4.5 and 8.5 K with SC transition. The two sets of temperatures and pressures: 180 K at ambient pressure and 8.5 K around 10 GPa are the same as the characteristic transition temperatures and pressures of CO and SC transitions in the stoichiometric β-$Li_{0.33}V_2O_5$, respectively. This suggests that the non-stoichiometric β-$Li_{0.38}V_2O_5$ includes another phase responsible for both a CO transition at 220 K under ambient pressure and a SC transition at 4.5 K under 7.5–9.6 GPa in one sample crystal, in addition to the stoichiometric β-$Li_{0.33}V_2O_5$ phase. Such two phase mixture in q1D conductor can explain the coexistence of two SC phases (β phase and another phase) around 10 GPa. Here it should be emphasized that zero-resisitivity behavior has never been observed in the stoichiometric β-$Li_{0.33}V_2O_5$.

As a likely coexistence, the mixture of β and β' phases can be considered from the special situation that only ternary Li-V-O system can form both β and β' structures.[5,30] Other A-V-O systems (A=Na, Ag, Ca, Sr, Pb, and Cu) can take only β or β' structure.

The crystal structures of β and β' phases are illustrated in Fig. 16. In this figure, A-cation is represented as balls and V_2O_5 framework is shown as a polyhedra network. Panel (a) illustrates a projection along the b axis and (b) shows a cross section (the b plane) of each β and β' structure at the broken line in panel (a). As shown in panel (b), the structural difference between β and β' phases results from only different A-cation arrays in the common V_2O_5 tunnels. As the result, the stoichiometric composition of A cation in β' phase is two times larger than that of β phase, namely, ideal β' phase is represented as β'-$A_{2/3}V_2O_5$. These characteristics suggest a possible phase separation into β and β' phases in the case of excess Li content.

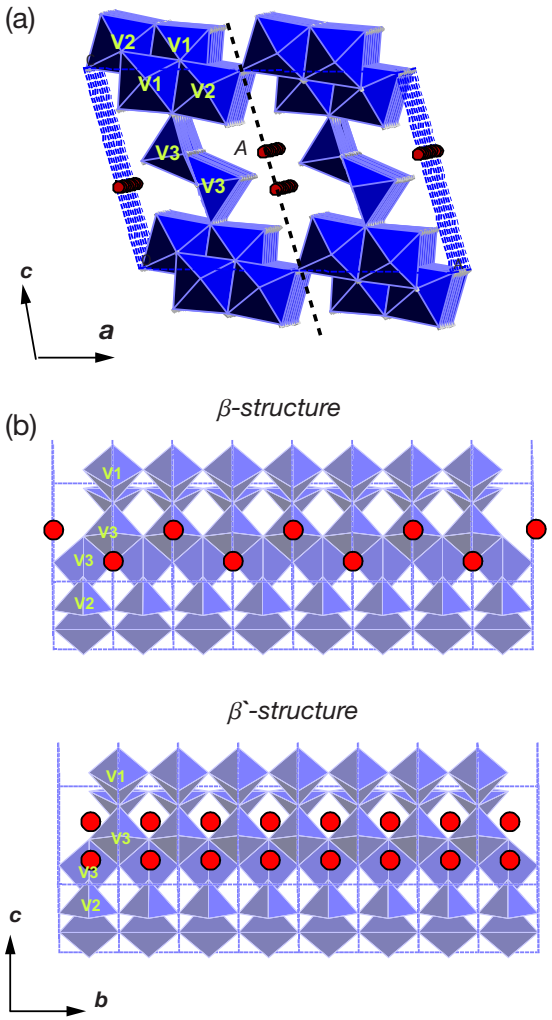

FIG. 16. (Color online) Crystal structures of β- and β'-vanadium bronzes. The cross section at the broken line in the upper panel (a) is shown in the lower panel (b) to demonstrate A-cation arrays in the V_2O_5 tunnels for each β and β' structure. The fact that only $Li_xV_2O_5$ system can form both structures and the similarity of both structures imply a possibility of coexistence of β and β' phases with the same V_2O_5 framework in β-$Li_{0.38}V_2O_5$ crystal with excess Li ions.

Actually, recent precise single crystal x-ray diffraction (XRD) and ^{7}Li-NMR measurements revealed the coexistence of two phases.[31,32] ^{7}Li-NMR reveals two sets of Li signal with clearly different local surroundings. On the other hand, powder XRD profile of β-$Li_{0.38}V_2O_5$ seems to be almost identical to that of β-$Li_{0.33}V_2O_5$ except slightly different d spacing. In such phase separation, each phase of the separated two phases might have a character of each stoichiometric end member, although the stoichiometric β' phase has never been synthesized under known conditions. Consequently, it is impossible to directly examine the properties of the stoichiometric pure β'-Li compound under ambient and high pressures. However, there is a good example from which we can analogize the properties of the stoichiometric pure β' phase. That is β'-$Cu_{0.65}V_2O_5$.

3. β'-$Cu_{0.65}V_2O_5$

A ternary Cu-V-O system can form β' structure and we can control Cu ion content in β'-$Cu_xV_2O_5$ system up to $x=0.65$, very close to the stoichiometric composition 0.66.[33] $x=0.65$ is the closest composition to the stoichiometric one, which can be prepared under ambient synthetic conditions. The nominal carrier number of β'-$Cu_{0.65}V_2O_5$ is almost the same as that of stoichiometric divalent β-$A_{0.33}V_2O_5$ (A=Ca, Sr, and Pb). In this Cu compound, pressure-induced superconductivity was discovered at about 5 K and at 4.5 GPa.[26] This fact gives some validity to the superconductivity in β'-Li phase under pressure.

As a common feature of β- and β'-vanadium bronzes, nonstoichiometry of A cations spoils its q1D metallic property. In the case of β'-Cu system, the metallic features are not so sensitive to off stoichiometry compared to the β phases. At $x=0.60$, metallic behaviors on ρ-T curves disappear. Note that all β-vanadium bronzes (A=Li, Na, Ag, Ca, Sr, and Pb) lose its metallic nature even in $x=0.32$.

Single crystals of β'-$Cu_{0.65}V_2O_5$ were grown and high-pressure experiments were carried out by using the crystals. Here, in Fig. 17(a), we show the ρ-T curves of a $x=0.65$ crystal along the b axis up to 6.5 GPa which also appeared in Ref. 26 The inset of this figure is an enlarged graph of the low-temperature part below 30 K. This compound does not show distinct MIT at ambient pressure but has a crystallographic transition at around the temperature with a hump of the ρ-T curve. The XRD study claimed the occurrence of partial charge ordering (PCO) at this transition.[34] The most intriguing aspect is a clear drop in the ρ-T curves at 3.0 and 4.5 GPa, as clearly seen in the inset. The drops appear at around 6 K; however, the ρ-T curves do not show zero resistivity (down to 35% of the onset in the ρ-T curve of 4.5 GPa). As further increase of pressure up to 6.5 GPa, the drop readily disappears. Note that such moderate drops in ρ-T curves have been frequently observed in β-vanadium bronzes near the critical pressure P_c where a SC phase begins to appear in a CO phase.

In order to confirm the pressure-induced SC phase, ac-susceptibility measurement was also performed under high pressure with the same method employed in β-Na compound. The obtained temperature dependence of the ac-susceptibility, $\chi(\omega)$-T curves ($\omega \sim 534$ Hz) at 4.0 and 4.5 GPa are also shown in Fig. 17(b). A clear drop in $\chi(\omega)$-T curve was observed at 4 K in 4.5 GPa, which was in good agreement with the results of resistivity measurements under pressure. Judging from the extremely low sensitivity of this ac-susceptibility measurement, only SC transition is a likely explanation for the drop in $\chi(\omega)$-T curve. Therefore this ac-susceptibility measurement strongly supports a pressure-induced SC phase in β'-$Cu_{0.65}V_2O_5$. The SC volume fraction was nominally estimated at about 6% as discussed above.

The SC signal on $\chi(\omega)$ is quite smaller ($\sim 1/10$) than that in β-Na compound. Such a small signal is consistent with non-zero-resistivity behavior in ρ-T curves. These poor SC properties are possibly attributed to the quality of crystal, namely, a slight off stoichiometry of Cu ions. However, the superconductivity observed in β'-$Cu_{0.65}V_2O_5$ justifies that

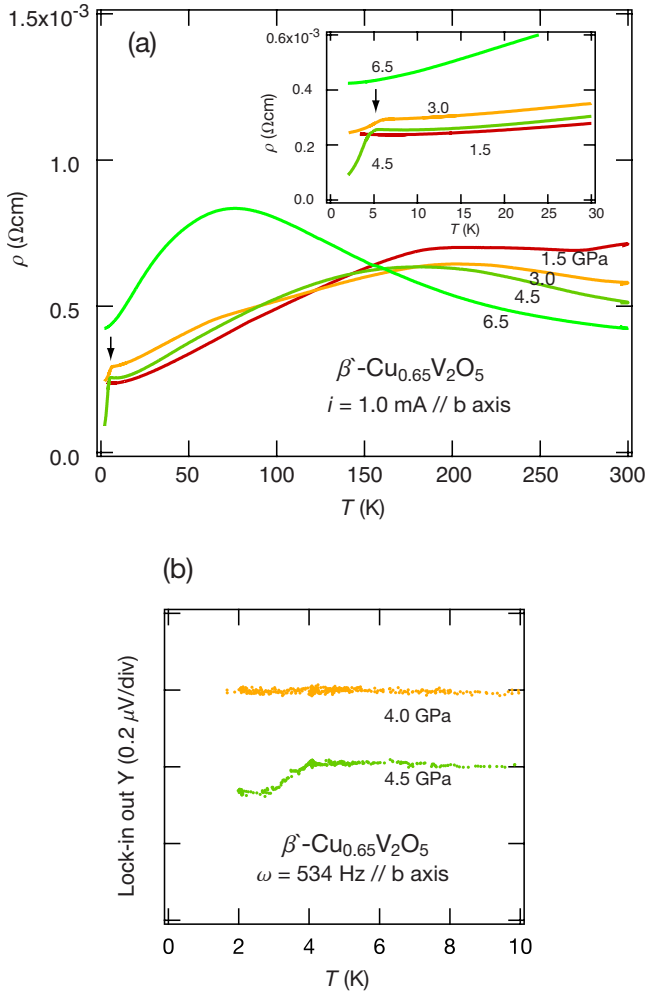

FIG. 17. (Color online) (a) ρ-T curves under pressure up to 6.5 GPa, which was also shown in Ref. 26 and (b) $\chi(\omega)$-T curves at 4.0 and 4.5 GPa for β'-$Cu_{0.65}V_2O_5$. The inset in panel (a) is simply a macrograph of the ρ-T curves under 30 K.

the second phase in the two phase mixture of β-$Li_{0.38}V_2O_5$ is possibly β'-$Li_{0.66}V_2O_5$ with a SC nature under high pressure.

4. P-T phase diagrams of β-$Li_{0.38}V_2O_5$ and β'-$Cu_{0.65}V_2O_5$

Many complex aspects observed in "overdoped" β-$Li_{0.38}V_2O_5$ are summarized as a P-T phase diagram exhibited in Fig. 18. In this phase diagram, several kinds of anomalies, MIT jump, kink, and SC drop in ρ-T curves are represented by filled and open small square and/or circle symbols which also appeared in Figs. 14 and 15.

These anomalies can be divided into two groups: the identical ones observed in the stoichiometric compound and the others. The former marked by filled symbols is attributed to the stoichiometric β phase, while the latter shown by open symbols could be responsible for the β' phase.

To demonstrate the sudden rise of T_{SC} with slight increasing pressure, 9.6–9.9 GPa, the phase diagram around the SC phase is enlarged as an inset. Here, the lower and higher T_{SC} are about 4.5 and 8.5 K, respectively. The SC phase with T_{SC}=4.5 K plotted by open circles is absent in the stoichiometric compound. The notation "SC+CO" in the hatched area means the coexistence of CO phase (β phase) and SC phase (β' phase). Note SC+CO region spreads over relatively wide pressure about 2 GPa compared with that (<1.0 GPa) in the stoichiometric compound.

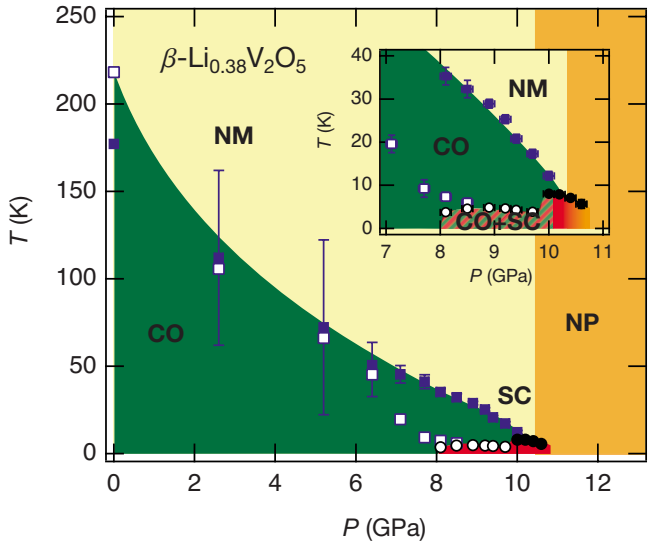

FIG. 18. (Color online) The P-T phase diagram of β-$Li_{0.38}V_2O_5$. Note the common meanings of the notations: CO, SC, NM, NP, and CO+SC. The inset is an enlarged picture around the SC phase in the main panel.

Just above the pressure of 9.6 GPa where T_{SC} suddenly rises up to 8.5 K, only one ρ-T curve at 10.1 GPa shows zero resistivity within the experimental resolution. This can be understood that both β and β' phases become to show SC nature at this pressure and the whole electronic path is connected by SC phases. With further slight increasing pressure up to 10.4 GPa, the NP phase probably appears and breaks SC phase as observed in the stoichiometric Li compound.

On the analogy of the phase relations in the stoichiometric β compound, the pure β'-Li compound probably has both CO and SC phases with a phase relation shown by two anomalies marked with open squares and circles. In this phase diagram, the phase boundary between CO and NM phases is drawn as the interpolation between anomalies at ambient and above 6 GPa, even though there is no distinct anomaly on the ρ-T curves in the pressure range 2.0–5.5 GPa. The large error bars in this pressure region are due to such uncertainty.

A P-T phase diagram of β'-$Cu_{0.65}V_2O_5$ is exhibited in Fig. 19, as a good reference to imagine the phase relation of β'-Li compound. The stoichiometric β'-Li compound, if it exists, is expected to show similar properties to this β'-Cu compound, because both compounds have common crystal structure and almost the same carrier number. The fact that β'-$Cu_{0.65}V_2O_5$ clearly shows pressure-induced superconductivity gives some validity to the superconductivity in β'-Li phase under pressure.

On the other hand, there are some different aspects between the properties of β'-Li compound deduced from the results of β-$Li_{0.38}V_2O_5$ and those of β'-Cu compound. The most significant one is the presence and/or absence of a dis-

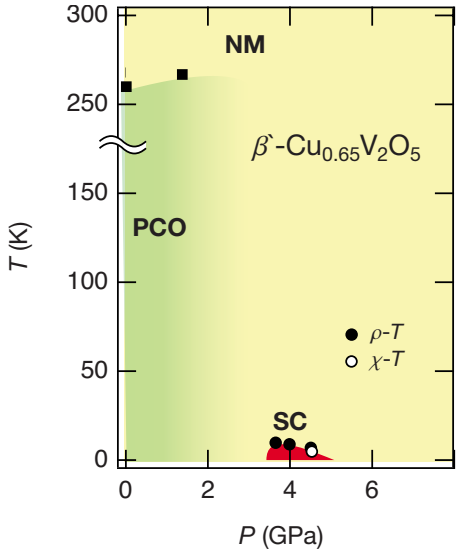

FIG. 19. (Color online) The P-T phase diagram of β'-$Cu_{0.65}V_2O_5$. The notation "PCO" denotes partial charge ordering phase (Ref. 34).

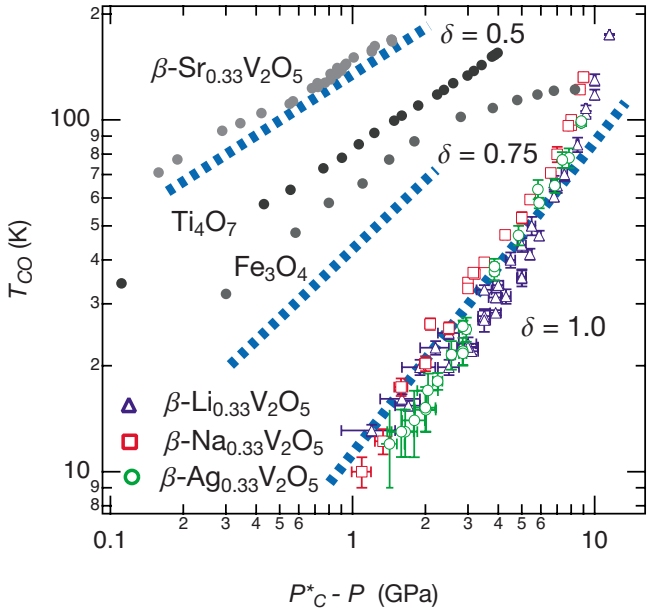

FIG. 20. (Color online) Pressure dependences of T_{CO} in β-$A_{0.33}V_2O_5$ (A=Li, Na, and Ag). The exponent δ is defined as $T_{CO} \propto (P_c^* - P)^{\delta}$, where P_c^* is defined as the pressure at T_{CO}=0 K (see the text). For comparison, the typical pressure dependences of T_{CO} in some other CO oxide compounds, Ti_4O_7, Fe_3O_4, and non-SC β-$Sr_{0.33}V_2O_5$, are also exhibited. Three broken lines are the guidelines of δ=0.5, 0.75, and 1.0.

tinct MIT (observed at 220 K in the overdoped Li compound at ambient) in β'-Li compound and/or β'-Cu compound. This difference seems to be crucial. However, it should be noted that the crystal structure transition (T_{PCO}=260 K) in β'-$Cu_{0.65}V_2O_5$ at ambient pressure has been discussed as a PCO phenomenon.[34] At present, the pressure dependence of T_{PCO} is observed only up to 1.5 GPa, showing the abrupt vanishing of a sign of the transition in ρ-T curves.

In this phase diagram, the filled square symbols denote T_{PCO}, and the filled and open circles show T_{SC} derived from ρ-T and $\chi(\omega)$-T curves, respectively. Although, unfortunately, the relation between SC and PCO phases is still unknown, it may be similar to that between CO and SC phases in the stoichiometric monovalent β-vanadium bronzes.

IV. DISCUSSION

A. Pressure dependence of T_{CO}

As shown in Fig. 11, CO phases in all monovalent stoichiometric β-vanadium bronzes are bounded by NM phases with rare concave shape in the P-T phase diagrams. Meanwhile various kinds of ordering states which are suppressed by pressure show a convex shape, for example, itinerant magnetic ordering[35] and Mott insulating phases.[36]

Although there is no established formalization to treat the pressure dependences of T_{CO}, we dare to employ the formalization discussed by Millis for magnetic ordering phase in itinerant fermion systems[37] to discuss the observed pressure dependences of T_{CO}. With an analogy between the charge degree of freedom on vanadium ions (V^{4+}/V^{5+}) and spin degree of freedom (spin up and/or down), the β-vanadium bronzes can be considered as spin systems in the formalization discussed by Watanabe.[38] In this formalization, magnetic transition temperature under pressure can be described as follows:

$$T_c(P) \propto (P_c^* - P)^{\delta}, \quad \delta \equiv \frac{z}{z+d-2}, \tag{1}$$

where the dynamic exponent, z, is expected to be z=3 in ferromagnetic (F) and z=2 in antiferromagnetic (AF) systems, and d represents spatial dimensionality of the system. Since the carrier d electrons should interact repulsively, it is natural to suppose z=2 in the case of β-vanadium bronzes.

To demonstrate pressure dependence of T_{CO}, we tried a log-log plot of T_{CO} versus $P_c^* - P$ (=ΔP), (T_{CO}-ΔP curves), for several kinds of compounds as shown in Fig. 20. In this plot, the exponent $\delta \equiv z/(z+d-2)$ for pressure dependence of T_{CO} is well represented as a slope of T_{CO}-ΔP curve as shown in this figure.

Here, it should be noted that the critical pressure, P_c^*, for monovalent β-vanadium bronzes is different from P_c in the previous sections. The P_c^* is defined as the pressure where T_{CO} becomes 0 K and it can be determined without some difficulty in ordinary cases. In the case of monovalent β-vanadium bronzes, however, SC phase suddenly appears at P_c before CO phase is completely suppressed, which makes the determination of P_c^* difficult. Then the P_c^* is determined so that the T_{CO}-ΔP curves in this log-log plot have the longest linear shapes. In other words, P_c^* is chosen in such a way that the the single exponent δ can describe the phase boundary between NM and CO phases as a wide pressure range as possible. The estimated critical pressures, P_c^*'s, for β-$A_{0.33}V_2O_5$ (A=Li, Na, and Ag) were 11.5 (Li), 9.0 (Na), and 8.8 GPa (Ag), respectively.

TABLE I. Simple calculations of exponent δ for ferromagnetic and antiferromagnetic cases in one- to three-dimensional systems using $\delta=z/(z+d-2)$. The δ was also calculated for one-dimensional system which was not discussed in the formalization of Millis.

System	AF ($z=2$)	F ($z=3$)
1D ($d=1$)	$\delta=2/(2+1-2)=2$	$\delta=3/(3+1-2)=3/2$
2D ($d=2$)	$\delta=2/(2+2-2)=1$	$\delta=3/(3+2-2)=1$
3D ($d=3$)	$\delta=2/(2+3-2)=2/3$	$\delta=3/(3+3-2)=3/4$

To show a peculiarity of monovalent β-vanadium bronzes, the pressure dependences of T_{CO} are also exhibited in Fig. 20 for some other CO oxides, Ti_4O_7,[39,40] Fe_3O_4,[41] and nonsuperconducting β-$Sr_{0.33}V_2O_5$.[42] The critical pressures, P_c^*'s, for these compounds were naturally estimated at 2.13 (Ti_4O_7), 8.3 (Fe_3O_4), and 1.46 GPa (β-Sr) in an ordinary way from the literatures.

In Fig. 20, three broken lines are also drawn as the guidelines of $\delta=0.5$, 0.75, and 1.0. As clearly shown in this figure, there is a substantial difference in the exponents δ among the compounds: $\delta\sim1.0$ for monovalent β-vanadium bronzes and $0.75>\delta>0.5$ for others. The δ is a quantity which relates to effective dimension of the system, expressed as $\delta=z/(z+d-2)$. In Table I, simple calculation data of δ are exhibited for one to three-dimensional ($d=1\sim3$) systems with F and AF ($z=3$ and 2) interactions. From the calculation, one can expect that both 2D F and AF systems are likely to show $\delta=1$, while three-dimensional (3D) systems could have smaller δ than $3/4=0.75$. It should be noted that 1D system was not discussed in the formalization of Millis. However, we also give the δs for 1D systems in Table I.

The result that the data points of all monovalent β-vanadium bronzes are scattered around $\delta=1$ line implies that they are 2D system, regardless of F and AF cases, namely, they are governed by 2D charge fluctuation. This also suggests that such 2D charge fluctuation is a possible origin of the superconductivity under high pressure in all monovalent β-vanadium bronzes. More over, one can also find two expectable δ's for 3D other compounds Ti_4O_7 and Fe_3O_4, and one peculiar δ for β-$Sr_{0.33}V_2O_5$. The later might be attributed to its complex P-T phase diagram.[42]

All β-vanadium bronzes show q1D conduction at ambient pressure; however, a pressure-induced dimensional crossover to q2D conduction was observed in divalent β-vanadium bronzes.[43] Furthermore, x-ray diffraction measurements under pressure revealed a relatively larger compliance along the a axis in β-$Na_{0.33}V_2O_5$, compared with other directions.[43,44] These facts allow us to suppose q2D conduction within the ab-plane under pressure, being consistent with the observed exponent δ.

B. $AT^2+\rho_0$ behaviors in normal states

The ρ versus T^2 curves for all stoichiometric monovalent compounds, β-$A_{0.33}V_2O_5$ (A=Li, Na, and Ag), near P_c and up to 70 K ($T^2=4900$ K^2) are exhibited in Fig. 21. All curves roughly show linear behaviors as $\rho=\rho_0+AT^2$ in a rather wide

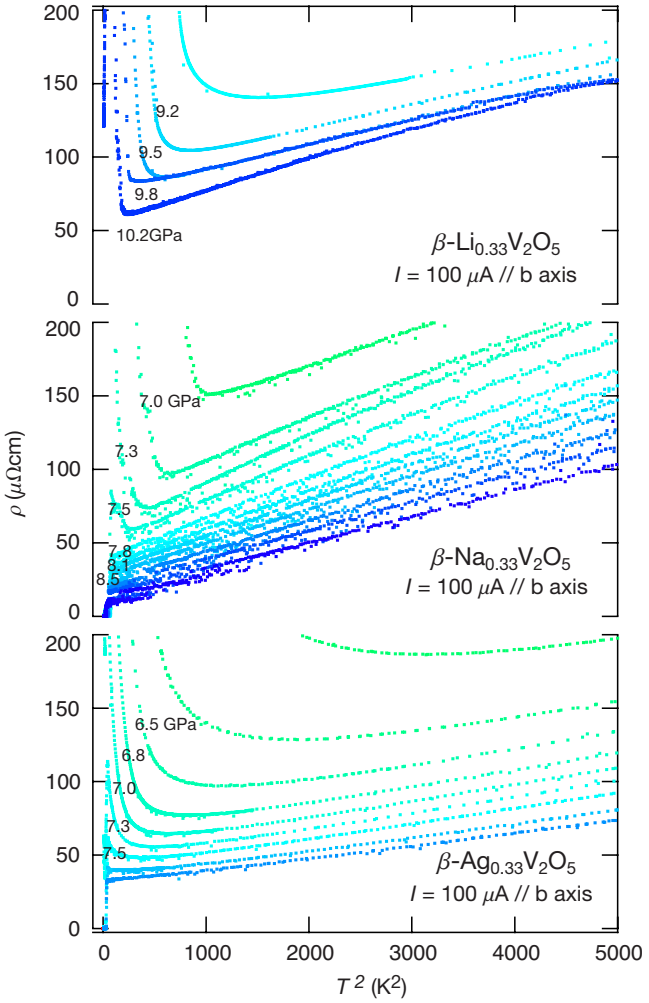

FIG. 21. (Color online) ρ-T^2 plots for all stoichiometric monovalent compounds near P_c up to 70 K ($T^2=4900$ K^2). The ρ-T^2 behaviors in the metallic phases of these compounds are observed in relatively wide pressure and temperature regions, indicating Fermi liquid nature. At the P_c, no drastic discrepancy from the T^2 behavior was observed.

temperature range, indicating their Fermi-liquid-like nature in the normal metallic phases. Non-Fermi-liquid-like conduction such as linear-T behavior in HTSC and ρ-$T^{3/2}$ curves observed near the quantum critical point (QCP) in heavy fermion system have not been observed; nevertheless, the systems are probably governed by 2D charge fluctuation as mentioned already.

The ρ-T^2 behaviors around P_c are observed in a considerably wide temperature range up to 50 K at least in Li compound and up to the highest 100 K in Na compound. Similar behaviors in the wide temperature range were observed in one typical early 3d-transition metal perovskite oxides, $La_xSr_{1-x}TiO_3$.[45] Such T^2 dependence of ρ in the wide temperature range reminds us of strong electron-electron scattering process rather than electron-phonon scattering process, in spite of the large electron-phonon coupling suggested in angle-resolved photoelectron spectroscopy study at ambient pressure.[46] These two observations at ambient and high pressures imply quite large pressure compliance of electron-

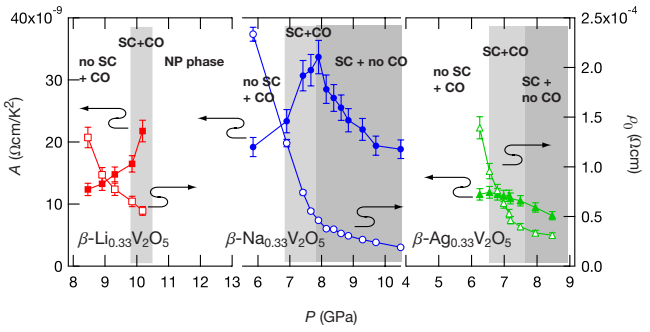

FIG. 22. (Color online) Pressure dependences of two parameters, residual resistivity ρ_0 and A coefficient of T^2 term. Both parameters were obtained by linear fitting in ρ-T^2 plot. The white, light, and dark gray backgrounds show the metallic regions with different ground states; CO phase without SC phase (white), coexistence of CO and SC phases (light gray), and SC phase without CO phase (dark gray), respectively. The white region of Li compound in the higher-pressure side corresponds to NP phase which breaks superconductivity.

electron (enhanced by pressure) and/or electron-phonon (suppressed by pressure) couplings.

Incidentally, since Fermi liquid is never realized in 1D system, the results strongly suggest that dimensional crossover from q1D to q2D or higher dimension occurs with applying pressure.

Typical values of the coefficient A of T^2 term at the P_c are 1.8×10^{-8} for Li compound, 2.3×10^{-8} for Na compound, and 1.2×10^{-8} Ω cm/K^2 for Ag compound, respectively. The A coefficients obtained in other early transition metal oxides are typically 2.0×10^{-6} Ω cm/K^2 for LiV_2O_4 (Ref. 47) and $(1.0-2.5)\times10^{-9}$ Ω cm/K^2 for $La_xSr_{1-x}TiO_3$.[45] Since the A coefficient is regarded as a measure of the electronic specific heat (γ), γ near the P_c in β-vanadium bronzes could be relatively larger than that in $La_xSr_{1-x}TiO_3$ (γ =8–16 mJ/K^2 mol) and considerably smaller than that in LiV_2O_4 (350–400 mJ/K^2 mol). The γ of monovalent β-vanadium bronzes near the P_c can be estimated at 30–55 mJ/K^2 mol, assuming the relation A/γ^2=constant $\sim1.0\times10^{-11}$ Ω cm(mol K^2/mJ)^2, which is frequently observed in highly correlated electron systems. The estimated γ values are relatively larger than those of typical $3d^1$-electron metallic vanadium oxides, $CaVO_3$ (7.3–8.6 mJ/K^2 mol) (Ref. 48) and β'-$Cu_{0.65}V_2O_5$ (13.6 mJ/K^2 mol) (Ref. 49) at ambient pressure.

The pressure dependences of two fitting parameters A and ρ_0 for all monovalent compounds are exhibited in Fig. 22. The linear fitting for each compound was carried out in the restricted pressure region where a linear relation of ρ-T^2 curves was realized. The white, light gray, and dark gray backgrounds in this figure represent the regions with CO, CO+SC, and SC ground states, respectively. The white region in the higher-pressure side for Li compound corresponds to NP phase which breaks both superconductivity and T^2 behavior. The most significant feature of this figure is that the pressure dependence of coefficient A (A-P curve) seems to have a peak at around P_c while the residual resistivity ρ_0 (ρ_0-P curve) monotonically decreases with increasing pressure. A clear peak of A-P curve was observed only in Na compound. We cannot know the behavior in the higher-pressure side than P_c for Li compound because it is probably masked by the NP phase. On the other hand, the region of T^2 dependence below P_c is too narrow to evaluate the behavior for Ag compound. However, such peak behavior of A-P curve is naturally expected in both Li and Ag compounds on the analogy of Na compound.

In the ordinary Fermi liquid picture, the coefficient of T^2 term, A, and residual resistivity, ρ_0 are proportional to $(m^*)^2$ and $1/lS_F$, respectively, where the m^*, l, and S_F are effective mass, meaning free path, and area of Fermi surface, respectively. Thus, A and/or ρ_0 are naturally expected to be relevant to T_{SC}. Actually several high-pressure studies have discussed A-P and ρ_0-P curves concerning the critical phenomena at the QCP.

A typical heavy fermion compound $CeCu_2Ge_2$ has been known to show characteristic pressure dependences; a substantial drop of A-P curve and a definite peak of ρ_0-P curve at the critical pressure $\sim$16 GPa. This compound is also a typical pressure-induced superconductor.[50] The superconductivity appears at $P>10$ GPa and at 0.6 K, and the T_{SC} is suddenly elevated to the maximum 2 K at 13–16 GPa. These anomalous behaviors, definite peak of ρ_0 and significant drop of A around the critical point (where the pressure dependence of T_{SC} shows a peak), have been interpreted as the change of the ground state degeneracy at the transition to intermediate valence state from Kondo state.[51] Moreover, some relations between the anomalies on ρ_0-P/A-P curves and the enhancement of T_{SC} have been argued in terms of valence fluctuation of Ce.[52]

Meanwhile, the SC pyrochlore oxide $Cd_2Re_2O_7$ shows somewhat different aspects on the ρ_0-P and A-P curves. Both ρ_0-P and A-P curves show unequivocal peak structures at P_c and these peaks are explained by structural phase transition between slightly different two phases.[53] The SC phase is confined in phase II which belongs to slightly distorted space group $F43m$. This space group slightly differs from the ideal pyrochlore space group $Fd\bar{3}m$ in phase I. As increasing pressure up to 3.5 GPa, phase II and the superconductivity disappear simultaneously. The peaks on both ρ_0-P and A-P curves were observed at this critical pressure. This phase transition has been argued as charger order uncoupled with MIT because Re^{5+} is relatively unstable in oxides and is expected to disproportionate into Re^{4+} and Re^{6+}. Furthermore, this disproportionation model can fairly explain the slightly distorted space group $F43m$ of the phase II.[53]

As seen in both compounds, $CeCu_2Ge_2$ and $Cd_2Re_2O_7$, various types of behaviors on A-P and ρ_0-P curves; peak, steep increasing, and decreasing, have been argued as critical phenomena concerning charge degree of freedom. All stoichiometric monovalent β-vanadium bronzes show similar behaviors; a peak of A-P curve and substantial decreasing of ρ_0-P at the P_c region. A significant characteristic of monovalent β-vanadium bronzes is the insulating-superconducting (IS) transition. Thus, the observed monotonic ρ_0 decreasing by a factor of 5 around P_c seems to be natural for the IS transition.

The relation $\rho_0 \propto 1/lS_F$ suggests considerable increasing of the S_F by a factor of 5 around P_c (l is naturally expected

to be constant with increasing pressure). On the other hand, the peak behavior of A-P curve demonstrates an enhancement of effective mass m^{*2} by a factor of 2 (Na compound) at P_c. Such enhancement of the coefficient A might be attributed to some increasing of the interaction between carriers via charge fluctuation near P_c. These anomalous behaviors in both A-P and ρ_0-P curves are intriguing to be explored because they could have a close relation to the appearance of superconductivity.

The most noteworthy aspect is that the superconducting transition temperatures T_{SC} decrease with increasing pressure even though ρ_0 decreases, namely, S_F probably increases with pressure. This feature strongly implies that the superconductivity is not BCS type. Moreover, T_{SC} as a function of pressure seems to scale to $A \propto (m^*)^2$, meaning that the correlation between electrons is an important parameter for T_{SC}.

C. Competition of various ground states under pressure

Pressure-induced SC phases adjacent to CO phases were observed in all monovalent β-vanadium bronzes, β-$A_{0.33}V_2O_5$ (A=Li, Na, and Ag) which were strictly tuned to the stoichiometric A-cation composition. In contrast, any SC phase was not observed in all divalent β-vanadium bronzes, β-$A_{0.33}V_2O_5$ (A=Ca, Sr, and Pb), although they became enough metallic under pressure.[44]

These experimental results seemed to lead to an idea that the carrier concentration of $V^{4+}(3d^1)/V=1/6$ would be crucial for the superconductivity in β-vanadium bronzes. However, a fact that almost stoichiometric β'-$Cu_{0.65}V_2O_5$ and probably β'-$Li_{0.66}V_2O_5$ show the superconductivity under pressure enables us to search for another factor for the presence and/or absence of superconductivity, because these compounds have almost the same carrier concentration of 1/3 as in divalent β-vanadium bronzes and have a common V_2O_5 framework responsible for their electromagnetic states.

Here, note that the SC phase collapses at 12 GPa in Na compound and just above 10 GPa in Li compound. These results are due to the appearance of new non-SC higher pressure phases (NP phase). The absence of superconductivity in divalent β-vanadium bronzes might be considered to be due to a similar phase relation, that is, the appearance of such new non-SC phase instead of SC phase. Actually we have observed an evidence or a sign of high-pressure phase in β-$Sr_{0.33}V_2O_5$ (Ref. 42) and β-$Pb_{0.33}V_2O_5$.[54]

In Sr compound, a non-SC new phase was actually discovered under high pressure.[42] This new phase borders on the CO and NM phases, showing the tricritical point around 100 K and 1.1 GPa. As a result, the NM phase is not stabilized down to the lowest temperature in Sr compound. Moreover, Pb compound shows an antiferromagneticlike order at 54 K under 0.4 GPa and this ground state survives at least up to 1.3 GPa.[54] Although it is still unclear whether the higher-pressure phase in Sr compound is magnetic ordering phase or not, such a high-pressure phase could be responsible for the absence of superconductivity.

D. Commensurability of carriers

As a characteristic of β-vanadium bronzes, the CO phases are steeply suppressed by introducing off stoichiometry. For example, ρ-T curve of β-$A_{0.30}V_2O_5$ crystal does not show any anomaly of MIT, while MIT still remains in β-$A_{0.32}V_2O_5$ compound. The SC phase is more sensitive to off stoichiometry than CO phase, because it disappears even in β-$A_{0.32}V_2O_5$ compound. A similar sensitive nature of superconductivity has been observed in Sr_2RuO_4, which has been discussed in the light of sample cleanliness as described in the Sec. III B 1. On the other hand, another factor might be considered in β-vanadium bronzes.

The fact that both charge order and superconductivity are quite sensitive to the stoichiometry suggests that a commensurability of carrier concentration is a crucial factor for the electromagnetic properties in β-vanadium bronzes, although the sensitivity to the off-stoichiometry is slightly different between charge order and superconductivity. This may imply a pronounce physics of commensurability for the superconductivity beyond the simple scenario of sample cleanliness for Sr_2RuO_4.

Recently the nature of the quantum valence transition in 1D periodic Anderson model with Coulomb repulsion between f and conduction electrons has been theoretically treated by the density-matrix renormalization group method. It reveals that the first-order valence transition emerges with QCP and the crossover from the Kondo to the mixed-valence states is strongly stabilized by quantum fluctuation and electron correlation. It is also found that the SC correlation is developed in the Kondo regime near the sharp valence transition.[55] Furthermore, a significant larger SC correlation can be expected in fractional carrier density systems.[56]

At present, it is difficult to say which effect, commensurability or cleanliness, is more crucial for the superconductivity of β-vanadium bronzes. To investigate a system with ion exchange such as $Na \leftrightarrow Ag$ might be effective to evaluate a role of carrier commensurability or cleanliness.

E. Electron-lattice coupling

In general, CO transitions observed in transition metal oxides are first-order transitions mainly because of strong couplings between charge and lattice degree of freedoms. In this sense, all the CO transitions in β-vanadium bronzes have first-order-like nature at ambient pressure.[57] Under high pressure, very recent NMR and synchrotron x-ray diffraction studies have revealed that β-$Na_{0.33}V_2O_5$ does not show any bond alternation (superstructure with lattice modulations) but shows charge disproportionation above 3 GPa.[58,59] These results mean the electron-lattice coupling should vary with increasing pressure. Ideally, the CO transition of V^{4+} and V^{5+} ions without lattice modulation can be thought as second-order transition in the analogy of antiferromagnetic ordering transition because the system can be easily mapped into spin up and down systems. Therefore, it is naturally expected that the CO transition becomes second-order with increasing pressure from first-order at ambient.

Actually we observed that large hysteresis of ρ-T curve at the CO transition becomes narrow as increasing pressure in β-$Li_{0.33}V_2O_5$. In the present study, however, it was difficult to observe strictly the variation of order of the CO transition under pressure and also the end point of first-order phase

TABLE II. Summary of the superconducting β- and β'-vanadium bronzes. The parameters, T_{CO}, P_c, and T_{SC} mean charge ordering temperature at ambient pressure, critical pressure, and optimum superconducting transition temperature, respectively.

	V^{4+}/V^{5+}	P_c (GPa)	T_{SC} (K)	Remarks
β-Li	1/5	9.9	8.5	$dT_{SC}/dH=-0.74$ K/T
β-Na	1/5	7.0	8.0	SC breaks at 12 GPa
β-Ag	1/5	6.8	6.5	
β'-Li	2/4	8.0	4.5	No single phase
β'-Cu	2/4	4.0	6.0	Partial CO?

boundary followed by second-order phase boundary in P-T phase diagrams. Here it should be noteworthy to introduce a fascinating theoretical prediction that SC correlation should be enhanced near such end point.[55,56]

To observe any contrast between V^{4+} and V^{5+} ions and their ordering structure above 3 GPa, more extensive works are needed in β-vanadium bronzes. The lattice modulationless charge order, namely, Wigner crystallization of electrons itself, is enough interesting. Moreover, it is desirable to know what kind of insulating phase is in contact with the SC phase in the P-T phase diagram.

V. SUMMARY

To summarize the pressure-induced superconductivity in this paper, the typical parameters and remarks of superconducting β- and β'-vanadium bronzes are exhibited in Table II. The SC state as a ground state of metallic β- and β'-vanadium bronzes is realized by suppressing the CO ground state with applying pressure. The SC phases appear in all stoichiometric monovalent β-vanadium bronzes, β-$A_{0.33}V_2O_5$ (A=Li, Na, and Ag) and in β'-$Cu_{0.65}V_2O_5$ and probably in β'-$Li_{0.66}V_2O_5$ which has almost the same carrier numbers as in divalent β-vanadium bronzes, β-$A_{0.33}V_2O_5$ (A=Ca, Sr, and Pb).

These results suggest that all stoichiometric members of β- and β'-vanadium bronzes would have SC phases, if there were not any reason to prevent the superconductivity. Actually, the SC phase in Li compound is about to be collapsed by non-SC higher-pressure phase (NP phase). Specifically, other kinds of non-SC ground states appear in non-SC divalent compounds (A=Ca, Sr, and Pb) prior to the stabilization of the ambient metallic (NM) phases down to the lowest temperature.

P-T phase diagrams of monovalent compounds show peculiar concave boundary between CO and NM phases. This shape itself shows 2D charge fluctuation near the P_c^*. Furthermore, the observed crucial effects of the A-cation stoichiometry to the superconductivity imply an important role of commensurability of carrier density and/or cleanliness of the system for the superconductivity.

Around P_c, the $AT^2+\rho_0$ behaviors of ρ-T curves of NM phases demonstrate Fermi liquid nature. The estimated electronic specific heat (γ) from A coefficients is relatively large, 30–55 mJ/K^2 mol. The most interesting thing is that the superconducting transition temperatures T_{SC} decrease with increasing pressure despite the fact that ρ_0 decreases, namely, S_F probably increases with pressure. This implies that this superconductivity is not BCS type. Moreover, T_{SC} as a function of pressure seems to be proportional to $\sqrt{A}(\propto m^*)$. This aspect allows us to suppose that the correlation between electrons is an important parameter for T_{SC}. This tendency (large A gives higher T_{SC}) also seems to be consistent with T_{SC}s in all monovalent compounds.

ACKNOWLEDGMENTS

The authors thank H. Ueda, M. Isobe, N. Takeshita, C. Terakura, J. I. Yamaura, S. Watanabe, S. Nagai, K. Ohwada, H. Seo, Y. Uwatoko, and M. Itoh for experimental help and valuable discussions. This study was supported by a Grant-in-Aid for Scientific Research (No. 18104008) from the Japan Society for the Promotion of Science.

*yamauchi@issp.u-tokyo.ac.jp

[1] D. Jerome, *Organic Conductors* (Dekker, New York, 1994).
[2] D. Jaccard, K. Behnia, and J. Sierro, Phys. Lett. A **163**, 475 (1992).
[3] B. Raveau, *Crystal Chemistry of High-T_c Superconducting Copper Oxides* (Springer-Verlag, Berlin, 1991).
[4] H. Yamada and Y. Ueda, J. Phys. Soc. Jpn. **68**, 2735 (1999).
[5] H. Yamada, thesis, University of Tokyo, 1999.
[6] M. Itoh, N. Akimoto, H. Yamada, M. Isobe, and Y. Ueda, J. Phys. Soc. Jpn. **69**, 155 (2000).
[7] S. Nagai, M. Nishi, K. Kakurai, Y. Oohara, H. Yoshizawa, H. Kimura, Y. Noda, B. Grenier, T. Yamauchi, J. I. Yamaura, M. Isobe, Y. Ueda, and K. Hirota, J. Phys. Soc. Jpn. **74**, 1297 (2005).
[8] T. Suzuki, I. Yamauchi, M. Itoh, T. Yamauchi, and Y. Ueda, Phys. Rev. B **73**, 224421 (2006).
[9] M. Itoh, I. Yamauchi, T. Kozuka, T. Suzuki, T. Yamauchi, J. I. Yamaura, and Y. Ueda, Phys. Rev. B **74**, 054434 (2006).
[10] J. Kikuchi (private communication). The ^{51}V NMR spectra down to 5 K on powder sample of β-$Pb_{0.33}V_2O_5$ do not show any splitting behavior with decreasing temperature as observed in other β-vanadium bronzes.
[11] T. Yamauchi, Y. Ueda, and N. Môri, Phys. Rev. Lett. **89**, 057002 (2002).
[12] A. D. Wadsley, Acta Crystallogr. **8**, 695 (1955).
[13] J. Galy, A. Casalot, and J. B. Goodenough, J. Solid State Chem. **1**, 339 (1970).
[14] T. Yamauchi, M. Isobe, and Y. Ueda, Solid State Sci. **7**, 874 (2005).
[15] Critical conductance represented as $G_c \sim e^2/\hbar(n/k_F^2)$ where $k_F l \sim 1$, and k_F and l show Fermi wave number and meaning free path of the carriers, respectively. At this conductance, the carri-

ers experience scattering events within the Fermi wavelength $\lambda_F = 2\pi/k_F$.
[16] Patrick A. Lee and T. V. Ramakrishnan, Rev. Mod. Phys. **57**, 287 (1985).
[17] Y. Ando, A. N. Lavrov, S. Komiya, K. Segawa, and X. F. Sun, Phys. Rev. Lett. **87**, 017001 (2001).
[18] Y. Fukuzumi, K. Mizuhashi, K. Takenaka, and S. Uchida, Phys. Rev. Lett. **76**, 684 (1996).
[19] M. Uehara, T. Nagata, J. Akimitsu, H. Takahashi, N. Môri, and K. Kinoshita, J. Phys. Soc. Jpn. **65**, 2764 (1996).
[20] D. Braithwaite, T. Nagata, I. Sheikin, H. Fujino, J. Akimitsu, and J. Flouquet, Solid State Commun. **114**, 533 (2000).
[21] T. Nakanishi, N. Motoyama, H. Mitamura, N. Takeshita, H. Takahashi, H. Eisaki, S. Uchida, and N. Môri, Phys. Rev. B **72**, 054520 (2005).
[22] M. J. Naughton, I. J. Lee, P. M. Chaikin, and G. M. Danner, Synth. Met. **85**, 1481 (1997).
[23] G. Knebel, D. Aoki, D. Braithwaite, B. Salce, and J. Flouquet, Phys. Rev. B **74**, 020501(R) (2006).
[24] T. Vuletić, P. Auban-Senzier, C. Pasquier, S. Tomić, D. Jórome, M. Héritierand, and K. Bechgaard, Eur. Phys. J. B **25**, 319 (2002).
[25] C. A. Kuntscher, S. Frank, I. Loa, K. Syassen, T. Yamauchi, and Y. Ueda, Phys. Rev. B **71**, 220502(R) (2005).
[26] Y. Ueda, M. Isobe, and T. Yamauchi, J. Phys. Chem. Solids **63**, 951 (2002).
[27] N. Kikugawa, C. Bergemann, A. P. Mackenzie, and Y. Maeno, Phys. Rev. B **70**, 134520 (2004).
[28] A. P. Mackenzie, R. K. W. Haselwimmer, A. W. Tyler, G. G. Lonzarich, Y. Mori, S. Nishizaki, and Y. Maeno, Phys. Rev. Lett. **80**, 161 (1998).
[29] N. Kikugawa and Y. Maeno, Phys. Rev. Lett. **89**, 117001 (2002).
[30] J. Galy, J. Solid State Chem. **100**, 229 (1992).
[31] M. Itoh (private communication). Comparing Li NMR spectra in both β-$Li_{0.33}V_2O_5$ and β-$Li_{0.38}V_2O_5$. Additional lines are clearly observed only in $x=0.38$ crystals.
[32] J. I. Yamaura (private communication). Precise single crystal XRD measurements demonstrate twining property of the crystals. This suggests macroscopic phase separation of β and β' phases.
[33] H. Yamada and Y. Ueda, J. Phys. Soc. Jpn. **69**, 1437 (1999).
[34] J. I. Yamaura, T. Yamauchi, M. Isobe, H. Yamada, and Y. Ueda, J. Phys. Soc. Jpn. **73**, 914 (2004).
[35] S. R. Julian, F. V. Carter, F. M. Grosche, R. K. W. Haselwimmer, S. J. Lister, N. D. Mathur, G. J. McMullan, C. Pfleiderer, S. S. Saxena, I. R. Walker, N. J. W. Wilson, and G. G. Lonzarich, J. Magn. Magn. Mater. **177-181**, 265 (1998).
[36] D. B. McWhan, A. Menth, J. P. Remeika, W. F. Brinkman, and T. M. Rice, Phys. Rev. B **7**, 1920 (1973).
[37] A. J. Millis, Phys. Rev. B **48**, 7183 (1993).
[38] S. Watanabe (private communication). There is no strict discussion that charge degrees of freedom can be mapped into spin up and down system. However, charge ordering patterns of some mixed-valence compounds were discussed as Ising spin systems, e.g., α'-NaV_2O_5, K. Ohwada *et al.*, Phys. Rev. Lett. **87**, 086402 (2001).
[39] H. Ueda, K. Kitazawa, H. Takagi, and T. Matsumoto, J. Phys. Soc. Jpn. **71**, 1506 (2002).
[40] N. Takeshita and H. Ueda (private communication).
[41] S. Todo, N. Takeshita, T. Kanehara, T. Mori, and N. N. Môri, J. Appl. Phys. **89**, 7347 (2001).
[42] T. Yamauchi, H. Ueda, J. I. Yamaura, and Y. Ueda, Phys. Rev. B **75**, 014437 (2007).
[43] T. Yamauchi, H. Ueda, K. Ohowada, J. I. Yamaura, and Y. Ueda (unpublished).
[44] J. I. Yamaura (private communication).
[45] Y. Tokura, Y. Taguchi, Y. Okada, Y. Fujishima, T. Arima, K. Kumagai, and Y. Iye, Phys. Rev. Lett. **70**, 2126 (1993).
[46] K. Okazaki, A. Fujimori, T. Yamauchi, and Y. Ueda, Phys. Rev. B **69**, 140506(R) (2004).
[47] C. Urano, M. Nohara, S. Kondo, F. Sakai, H. Takagi, T. Shiraki, and T. Okubo, Phys. Rev. Lett. **85**, 1052 (2000).
[48] I. H. Inoue, C. Bergemann, I. Hase, and S. R. Julian, Phys. Rev. Lett. **88**, 236403 (2002).
[49] T. Yamauchi and M. Nohara (unpublished). Specific-heat measurements were conducted by relaxation method in β'-$Cu_{0.65}V_2O_5$ which is the only metallic compound to the lowest temperature in a series of β-vanadium bronzes. It revealed 13.6 mJ/K^2 mol as a γ.
[50] D. Jaccard, H. Wilhelm, K. Alami-Yadri, and E. Vargoz, Physica B **259-261**, 1 (1999).
[51] A. T. Holmes, D. Jaccard, and K. Miyake, Phys. Rev. B **69**, 024508 (2004).
[52] K. Miyake, O. Narikiyo, and Y. Onishi, Physica B **59-261**, 676 (1999); Y. Onishi and K. Miyake, J. Phys. Soc. Jpn. **69**, 3955 (2000).
[53] Z. Hiroi, T. Yamauchi, T. Yamada, M. Hanawa, Y. Ohishi, O. Shimomura, M. Abliz, M. Hedo, and Y. Uwatoko, J. Phys. Soc. Jpn. **71**, 1553 (2002).
[54] T. Yamauchi, H. Ueda, J. Kikuchi, and Y. Ueda, J. Phys. Soc. Jpn. **76**, Suppl. A, 122 (2007).
[55] S. Watanabe, M. Imada, and K. Miyake, J. Phys. Soc. Jpn. **75**, 043710 (2006).
[56] S. Watanabe (private communication). Very recent first principles calculations demonstrated that the SC correlation is developed at the Kondo regime near the sharp valence transition, particularly in fractional carrier density systems.
[57] J. I. Yamaura, M. Isobe, H. Yamada, T. Yamauchi, and Y. Ueda, J. Phys. Chem. Solids **63**, 957 (2002).
[58] K. Ohowada, Y. Fujii, and Y. Murakami (private communication). In SPring-8 synchrotron radiation facility using DAC, they observed steep disappearing of superstructure of lattice even at 3 GPa, even though MI transition was clearly observed at this pressure.
[59] M. Itoh, T. Kozuka, I. Yamauchi, and T. Suzuki (private communications). Up to at least 6 GPa, they observed characteristic NMR spectra of charge disproportionation in this compound. This probably means an occurrence of charge ordering with quite small (invisible in x-ray diffraction measurements) lattice displacements.